

Implementation and Learning of Quantum Hidden Markov Models

Vanio Markov,¹ Vladimir Rastunkov,² Amol Deshmukh,² Daniel Fry,² and Charlee Stefanski¹

¹*Wells Fargo*

²*IBM Quantum, IBM Research*

(Dated: February 27, 2025)

In this article, we use the theory of quantum channels and open quantum systems to provide an efficient unitary characterization of a class of stochastic generators known as quantum hidden Markov models (QHMMs). By utilizing the unitary characterization, we demonstrate that any QHMM can be implemented as a quantum circuit with mid-circuit measurement. We prove that QHMMs are more compact and more expressive definitions of stochastic process languages compared to the equivalent classical hidden Markov models (HMMs). Starting with the formulation of QHMMs as quantum channels, we employ Stinespring's construction to represent these models as unitary quantum circuits with mid-circuit measurement. By utilizing the unitary parameterization of QHMMs, we define a formal QHMM learning model. The model formalizes the empirical distributions of target stochastic process languages, defines hypothesis space of quantum circuits, and introduces an empirical stochastic divergence measure - hypothesis fitness - as a success criterion for learning. We demonstrate that the learning model has a smooth search landscape due to the continuity of Stinespring's dilation. The smooth mapping between the hypothesis and fitness spaces enables the development of efficient heuristic and gradient descent learning algorithms.

We propose two practical learning algorithms for QHMMs. The first algorithm is a hyperparameter-adaptive evolutionary search. The second algorithm learns the QHMM as a quantum ansatz circuit using a multi-parameter non-linear optimization technique.

CONTENTS

		B. Classic Market Model with Four Hidden States	35
I. Introduction	2	VI. Conclusions and Outlook	36
II. Preliminaries	3	VII. Acknowledgements	36
A. Stochastic Languages and Hidden Markov Models	3	References	37
B. Quantum States and Quantum Operations	5		
III. Quantum Hidden Markov Models	10		
A. Unitary Definition of QHMM	15		
B. Primary and Measurement System Design. Test Case for the Ansatz Circuit Design	17		
IV. Learning Quantum Hidden Markov Models	20		
A. Empirical Specification of Stochastic Languages	20		
B. QHMM Hypotheses Space	22		
C. Quality of a Hypothesis	22		
1. Precision of a Hypothesis	22		
2. Complexity of a Hypothesis	24		
D. Formalization of the QHMM Learning Problem	24		
E. QHMM Learning Algorithm	26		
F. Learning QHMM with Ansatz Circuits	31		
G. Ansatz Circuit Template	32		
V. Examples of QHMMs	32		
A. Simple Four Symbol Stochastic Process	32		

I. INTRODUCTION

In this article we study quantum models of discrete stochastic processes. We assume that the processes are generated by *finitary* mechanisms with restricted memory and time. Furthermore, we assume that only subset of the process variables are observable, and the distributions of these observations are dependent on an underlying unobservable process. A common modeling approach for such situations is to use two joint stochastic processes: a latent state process, and a dependent output emission process. The state process is considered a stochastic Markovian process [1] with a finite number of "hidden" states. The observable process is represented as a probabilistic map from the hidden states to the symbols of a finite alphabet. Such a modeling framework is referred to as a *hidden Markov model* (HMM) [2].

Hidden Markov models are applicable in various real-world situations. The concept of latent variables is used to estimate circumstances and relations which are not directly observable. The assumption of underlying Markovian dynamics allows for the development of tractable learning and inference procedures. These models were introduced by Baum and Petri [3] in 1966, and since then have been successfully applied in areas such as linguistics [4–7], DNA analysis [8–10], engineering [11, 12], and finance [2, 13].

The *learning problem* for HMMs is to estimate the transition and emission operators of an unknown HMM given a finite sample of its emissions distributions. The conventional approach to solving the learning problem is based on maximization of observations' likelihood [3, 14–17]. Despite the fact that the expectation-maximization cannot be performed in polynomial time [18], this approach has been widely successful in practice [19]. Another group of learning algorithms, known as *spectral algorithms* [20–22] have polynomial time complexity. These algorithms represent the joint frequencies of the observed sequences as a matrix known as a Hankel matrix [20]. The rank of the matrix is used as an estimate of the order of the model. The model parameters are mapped to the factors of matrix's singular value decomposition. These learning algorithms belong to a specialized area known as *realization problem* for HMMs [20, 21].

The objective of this research is to propose a methodology for the physical implementation of quantum HMMs, as well as to develop practical learning algorithms for these models. Our approach is to *quantize* a classical HMM by replacing its stochastic vector space by the space of quantum density operators. The classical transition and emission operators are represented as *observable opera-*

tors [23] and replaced by *quantum operations*. A quantum operation, also known as *quantum channel*, is a linear, completely positive trace-preserving map (CPTP map) defined on the space of density operators [24]. When a quantum operation is used to quantize a classic HMM, it has two roles. Firstly, it defines the stochastic changes of model's state, representing the underlying Markovian process. Secondly, when interpreted as a *general measurement* (POVM) operator, the quantum operation describes the observable process.

The definition of a quantum hidden Markov model (QHMM) as a quantum operation was initially introduced by Monras et al. [25]. Since then, various aspects of QHMMs were studied by Srinivasan et al. [26–32], O'Neill [33], and Clark [34]. Javidian [35] discussed a different type of model called the circular QHMM. Cholewa et al. [36] studied HMMs based on quantum walks and transition operation matrices. Elliot [37] uses the concept of *memory compression* to demonstrate that the quantum HMMs achieve strict advantage compared to the corresponding classical HMMs. The memory compression is related to the size of the models' state-space and the amount of information it stores. Furthermore, other quantum approaches to sequence modeling are being proposed. For instance, Blank et al. [38] investigated characteristic function of discrete stochastic processes and proposed quantum algorithm for learning it, leveraging techniques such as quantum amplitude estimation and quantum Monte Carlo methods.

To implement QHMMs on quantum computers and develop feasible learning procedures, we employ the open quantum systems theory [24] and utilize Stinespring's dilation theorem [39] to derive unitary representation of the models. According to this theorem, every quantum operation can be represented as unitary evolution in an extended Hilbert space, followed by disregarding some degrees of freedom. We use this construction to parameterize any QHMM, defined by a quantum operation, as a unitary transformation in a larger Hilbert space. This parametrization enables the physical implementation of QHMMs as unitary quantum circuits with mid-circuit measurements. Furthermore, we exploit the continuity of Stinespring's procedure [40], to define a hypothesis space and corresponding learning objective, enabling efficient learning of QHMMs.

The main contributions of our study are

- We demonstrate that QHMMs are more *compact generators* of stochastic process languages compared to classical hidden Markov models. We show that if a QHMM generates a stochastic language of finite rank r , it requires only a Hilbert space of dimension at most $N = \sqrt{r}$.

In contrast, the minimal classical HMM for such a language, if the model exists, requires at least $n = r$ -dimensional classic vector space.

- We demonstrate that QHMMs are more *expressive generators* of stochastic process languages compared to classical hidden Markov models. For every stochastic language with finite rank r , there exists QHMMs \mathbf{Q} in Hilbert space with dimension $N = \lfloor \sqrt{r} \rfloor$. It is well known [41, 42], that there exist finite-rank stochastic languages which cannot be realized by classical QHMMs.
- For every QHMM defined as a quantum operation we provide an equivalent QHMM implementation as a unitary circuit with mid-circuit measurement.
- We provide a formal QHMM learning model formalizing the training data sample, hypothesis space of unitary quantum circuits, and hypothesis quality criteria as stochastic divergence between two distributions.
- We propose a tractable empirical distance measure between two QHMMs in terms of the divergence of their observable distributions. We prove that the empirical distance is dominated by the distance measure induced on the space of QHMMs by the diamond norm.
- We demonstrate that the landscape of the proposed QHMM learning model is smooth, which follows from the convergence properties of Stinespring’s dilation theorem [40]. The smooth landscape implies efficient heuristic and gradient-based learning algorithms.
- We specify a QHMM learning algorithm as adaptive evolutionary search in the space of quantum circuits with mid-circuit measurement.
- We specify a QHMM learning algorithm as multi-parameter nonlinear optimization in the space of pre-defined quantum ansatz.

This article is organized as follows:

- Section II presents some preliminary information regarding stochastic process languages, classic hidden Markov models and observable operators models. It introduces critical concepts including quantum states, quantum operations, general measurement and quantum mid-circuit computation.
- Section III presents the basic definition of a QHMM as quantum operation and provides

unitary definition of QHMMs and their implementation as quantum circuits with mid-circuit measurement.

- Section IV discusses a formal QHMM learning model defining data samples, hypothesis space and learning criterion. It specifies adaptive evolutionary and ansatz-based QHMM learning algorithms.
- Section V presents two examples: a market model and a stochastic volatility model.
- Section VI discusses our conclusion and outlook.

II. PRELIMINARIES

A. Stochastic Languages and Hidden Markov Models

We study a class of discrete time stationary stochastic processes,

$$\{Y_t : t \in \mathbb{N}, Y_t \in \Sigma\},$$

where $\Sigma = \{a_1, \dots, a_m\}$ is a finite set of observable symbols, called an *alphabet*. The set of all finite sequences over the alphabet Σ , including the empty sequence ϵ , is denoted by Σ^* . Finite sequences of symbols are denoted by the bold lowercase letters $\mathbf{a}, \mathbf{p}, \mathbf{s}$. The set of all sequences with length exactly t is denoted by Σ^t . For any $\mathbf{a} \in \Sigma^*$ let $|\mathbf{a}|$ be the number of symbols in the sequence. If \mathbf{p} and \mathbf{s} are sequences, then \mathbf{ps} denotes their *concatenation*. The sequence \mathbf{p} is called the *prefix* and \mathbf{s} is called the *suffix* of \mathbf{ps} . Any subset of Σ^* is a *language* L over the alphabet. The sequences belonging to a language are referred to as *words*. The set of sequences originated by observations or measurement of the evolution of a discrete-time process is called the *process language*. It is easy to verify that if a word results from the observation of a process, then every one of its subwords has also been observed. Therefore, the process languages are *subword-closed*.

A *stochastic* process language L is a process language together with a set

$$D^L = \{D_t^L : t \geq 0\} \quad (1)$$

of finite dimensional probability distributions D_t^L , each of which is defined on the sequences with length exactly t :

$$D_t^L = \{P[\mathbf{a}] : \mathbf{a} \in \Sigma^t, \sum_{\mathbf{a} \in \Sigma^t} P[\mathbf{a}] = 1\}. \quad (2)$$

The following properties of a stochastic process language are straightforward to prove:

- If the probability of a sequence \mathbf{p} is $P[\mathbf{p}]$, then the conditional probability to observe a symbol a after observing \mathbf{p} is

$$P[a \mid \mathbf{p}] = \frac{P[\mathbf{p}a]}{P[\mathbf{p}]}.$$

- Every stochastic language L and sequence of symbols $\mathbf{p} \in \Sigma^*$ define collections of distributions $P_t[\mathbf{s} \mid \mathbf{p}]$ over the sequences with equal length $t > 0$:

$$\sum_{\mathbf{s} \in \Sigma^t} P[\mathbf{p}\mathbf{s}] = P[\mathbf{p}], \forall \mathbf{p} \in \Sigma^*.$$

Two sequences \mathbf{p}_1 and \mathbf{p}_2 are called *t-equivalent* with respect to a stochastic language L if they define the same distribution over Σ^t :

$$P_t[\mathbf{s} \mid \mathbf{p}_1] = P_t[\mathbf{s} \mid \mathbf{p}_2], \forall \mathbf{s} \in \Sigma^t.$$

We study observable processes $\{Y_t : Y_t \in \Sigma\}$ where each observation Y_t depends on the state of a non-observable or *hidden* finite-state process $\{X_t : X_t \in S\}$, where $S = \{s_1, \dots, s_n\}$. The processes $\{Y_t\}$ and $\{X_t\}$ are called *emission process* and *state process* respectively. If the joint process $\{Y_t, X_t : t \in \mathbb{N}, Y_t \in \Sigma, X_t \in S\}$ is assumed to be stationary, then we can describe it by a linear model known as (classical) hidden Markov model (HMM). The model assumes *Markovian* evolution of the hidden state process $\{X_t\}$. The observed process $\{Y_t\}$ is emitted by a linear stochastic operator mapping the current hidden state to an observable symbol.

Definition 1 (Classical Hidden Markov Model). *A classical hidden Markov model is defined as a 5-tuple:*

$$\mathbf{M} = \{\Sigma, S, A, B, \mathbf{x}_0\}$$

where $\Sigma = \{a_1, \dots, a_m\}$ is a finite set of observable symbols, $S = \{s_1, \dots, s_n\}$ is a finite set of unobservable or hidden states and the number of states n is called the order of the model, A is a row-stochastic state transition matrix, B is a column-stochastic observations emission matrix, and \mathbf{x}_0 is a stochastic vector defining the initial superposition of the process' states.

At any moment in time t , the model is in a superposition (stochastic mixture) of its hidden states, described by a stochastic vector $x_t \in \mathbb{R}^n$. The component x_t^i represents the probability of being in state s_i .

The evolution of the hidden states follows a Markovian process defined by the transition matrix:

$$x_{t+1} = Ax_t.$$

At any moment in time t , the model defines symbol emission probabilities using a stochastic vector $y_t \in \mathbb{R}^m$, which depends on the current state x_t through the emission matrix B :

$$y_t = Bx_t.$$

The component y_t^i represents the probability of emitting symbol a_i . However, it's important to note that the evolution of the observation process, in general, is not a Markovian process.

The *steady state* of a stationary HMM is a stochastic vector \mathbf{x}^* defined as

$$\mathbf{x}^* = A\mathbf{x}^*.$$

The steady state \mathbf{x}^* is the eigenvector of the state transition operator A with eigenvalue 1, normalized to represent a probability distribution.

For every HMM \mathbf{M} we can define a set of *observable operators* \mathbf{T} as

$$\mathbf{T} = \{T_a : T_a = AB_a, a \in \Sigma\}, \quad (3)$$

where $B_a = \text{diag}(B[a, i]), i \in 1, \dots, n$ are diagonal matrices defining symbol observation probabilities for each state s_i [43, 44].

Every element of an observable operator T_a defines the conditional probability of the model being in state s_j if, at the previous moment in time, it was in state s_i and the symbol a was emitted.

$$T_a^{i,j} = P[s_j \mid s_i, a].$$

Let $\mathbf{a} = a_1 \dots a_t$ be any sequence. We define the observable operator corresponding to \mathbf{a} as follows:

$$T_{\mathbf{a}} = T_{a_t} \dots T_{a_1}.$$

For any sequences $\mathbf{a}, \mathbf{b} \in \Sigma^*$ the following composition of the observable operators is easy to verify:

$$T_{\mathbf{ab}} = T_{\mathbf{b}}T_{\mathbf{a}}.$$

The state transition operator A is related to the observable operators $\{T_a\}$ as follows:

$$A = \sum_{a \in \Sigma} T_a.$$

A Hidden Markov Model (HMM) \mathbf{M} defines the probability of every finite observable sequence $\mathbf{a} = a_1 \dots a_t$ as:

$$P[\mathbf{a} \mid \mathbf{M}] = \mathbf{1}T_{a_t} \dots T_{a_1}\mathbf{x}_0 = \mathbf{1}T_{\mathbf{a}}\mathbf{x}_0, \quad (4)$$

where $\mathbf{1}$ is the all-ones row vector with dimension n . With every model \mathbf{M} we associate a *sequence function* $f^{\mathbf{M}} : \Sigma^* \rightarrow [0, 1]$ defined as:

$$f^{\mathbf{M}}(\mathbf{a}) = P[\mathbf{a}|\mathbf{M}], \forall \mathbf{a} \in \Sigma^*. \quad (5)$$

Through its sequence function, every HMM \mathbf{M} defines a stochastic process language $L^{\mathbf{M}}$ consisting of a set of distributions for each $t \in \mathbb{N}$:

$$D_t^{\mathbf{M}} = \{f^{\mathbf{M}}(\mathbf{a}) : \mathbf{a} \in \Sigma^t\} \quad (6)$$

We compare HMMs based on the languages they define or generate. Two HMMs are considered *equivalent* if they define the same stochastic process language.

Let us assume that we have observed a process up to a certain moment in time t :

$$\mathbf{a} = a_1 \dots a_t.$$

The probability of the next symbol being a is given by:

$$\begin{aligned} P[a|\mathbf{a}] &= \frac{P[\mathbf{a}a]}{P[\mathbf{a}]} \\ &= \mathbf{1}T_a \frac{T_{\mathbf{a}}\mathbf{x}_0}{\mathbf{1}T_{\mathbf{a}}\mathbf{x}_0} \\ &= \mathbf{1}T_a\mathbf{x}_t, \end{aligned}$$

where

$$\mathbf{x}_t = \frac{T_{\mathbf{a}}\mathbf{x}_0}{\mathbf{1}T_{\mathbf{a}}\mathbf{x}_0}$$

is the stochastic mixture of states after the emission of the sequence \mathbf{a} .

For every HMM \mathbf{M} , let's consider a *bi-infinite* matrix, commonly referred to as a generalized *Hankel matrix*, defined by the sequence function (5) of the model [20]:

$$H^{\mathbf{M}} \in R^{\Sigma^* \times \Sigma^*}, H^{\mathbf{M}}[\mathbf{p}, \mathbf{s}] = f^{\mathbf{M}}(\mathbf{ps}), \forall \mathbf{p}, \mathbf{s} \in \Sigma^*, \quad (7)$$

where \mathbf{ps} denotes a concatenation of sequences \mathbf{p} and \mathbf{s} . We can say that $H^{\mathbf{M}}$ is indexed by the prefix \mathbf{p} and suffix \mathbf{s} of the sequence \mathbf{ps} . The rows of $H^{\mathbf{M}}$ are indexed by the prefixes \mathbf{p} in the *first lexicographical order*, and the columns are indexed by suffixes \mathbf{s} in the *last lexicographical order* of the sequences [20]. A sequence function $f^{\mathbf{L}}$ and the corresponding generalized Hankel matrix $H^{\mathbf{L}}$ are defined for every stationary stochastic language L by the distributions $D_t^{\mathbf{L}}$ (2):

$$f^{\mathbf{L}}(\mathbf{a}) = P[\mathbf{a}|D_t^{\mathbf{L}}], \forall \mathbf{a} \in \Sigma^t, \forall t \in \mathbb{N}. \quad (8)$$

The *rank* of a stochastic language is the rank of its Hankel matrix. This matrix is important, because its finite-rank property is a necessary condition for the stochastic language to have a HMM realization.

Theorem 1 (Anderson [20]). *If H is the infinite generalized Hankel matrix associated with a HMM \mathbf{M} of order n , then $\text{rank}(H) \leq n$.*

It has been proven [45], that the equality in **Theorem 1** can be reached, i.e. there exist minimal order n HMMs with $\text{rank}(H) = n$. If a HMM \mathbf{M} has order n its finite dimensional distributions $D_t^{\mathbf{M}}$ are completely defined by the values of the sequence function $f^{\mathbf{M}}(\mathbf{a})$ for all sequences \mathbf{a} of length at most $2n - 1$ [43, 44].

In general, not every finite-rank stochastic language has a HMM [46]. Determining whether a stochastic language L has finite rank is an undecidable problem [47].

Example 1. The evolution of asset prices on today's exchanges is driven by the interaction of ask and bid orders placed on an electronic two-sided queue known as a *Limit Order Book* (LOB) [48]. One important statistic associated with the LOB is the *mid-price*. The mid-price is the mean of lowest ask order price and highest bid order price at any given moment. In this example we present very simple HMM of the discrete-time mid-price direction of change.

At any given moment, the symbol $\mathbf{1}$ is observed if the price has increased, while the symbol $\mathbf{0}$ is observed if the price has decreased or remained unchanged. It is assumed that the distribution of observed directions of change depends on the underlying state of the market, which is not directly observable. Let us consider a very simple situation, where the market can be in one of four states: bear, bull, transition to bear, or transition to bull, as listed in Table I. The distribution of observation sequences is shown in FIG 1. The generalized Hankel matrix associated with the model has a rank of 4 for sequences containing up to 20 symbols. Therefore, we conclude that the order of this model is 4.

B. Quantum States and Quantum Operations

We study quantum models of discrete-time joint stochastic processes. These models assume two processes: an underlying, hidden Markov process that evolves in discrete time according to linear stochastic dynamics, and a second, observable process that produces an observation at each time step by applying a stochastic map to the hidden state. To quantize this model, it is necessary to define quantum concepts that correspond to its states, state evolution, observables, and the dynamics of the measurement process. The states of the process will be represented by the states of an n -qubit quantum system, where the associated complex Hilbert space \mathcal{H} [24]

s	Description
0	Bear - Tendency down
1	Bull - Tendency up
2	Transition to Bear
3	Transition to Bull

s	0	1	2	3
0	0.5	0.1	0.15	0.25
1	0.1	0.5	0.25	0.15
2	0.25	0.15	0.5	0.1
3	0.15	0.25	0.1	0.5

s	Symbol 0	Symbol 1
0	0.8	0.2
1	0.2	0.8
2	0.4	0.6
3	0.6	0.4

TABLE I. Left: Market hidden states descriptions. Center: State transition probabilities. Right: Observed symbol probabilities.

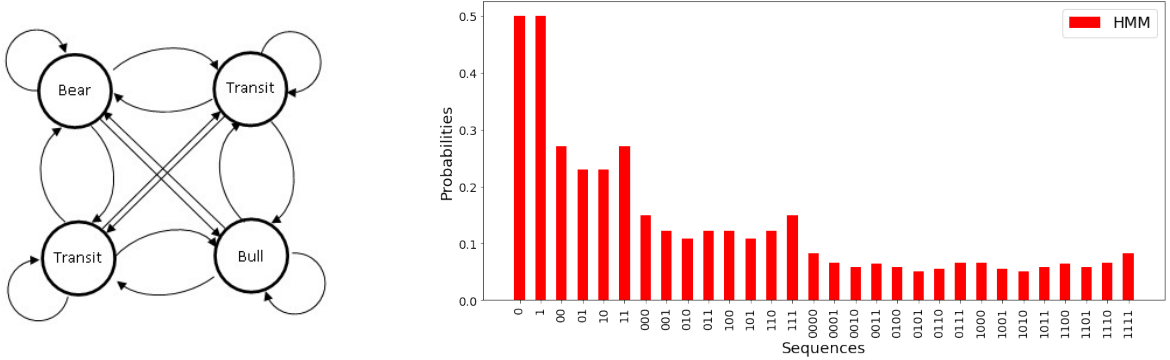


FIG. 1. Left: State transition graph. Right: Distribution of observed symbol sequences.

is a linear vector space with an inner product and dimension $N = 2^n$. The vectors of \mathcal{H} are denoted by $|v\rangle$. A complete description of the quantum system at any given moment in time is called a *quantum state*. When a quantum state is precisely determined, it is a *pure state*. The pure states are defined by *rays* in the space \mathcal{H} . The ray is an equivalence class of vectors that differ by multiplication by a nonzero complex scalar. Vectors within the same ray represent the same pure quantum state. Every ray is represented by a vector $|v\rangle$ with unit norm $\langle v|v\rangle = 1$. This normalization ensures that the representative vector captures the essential geometric properties and direction of the quantum state. To give a probabilistic interpretation of the pure states let's assume that $\{|x\rangle\}$ is an orthonormal basis in \mathcal{H} and any pure state $|v\rangle$ can be represented as

$$|v\rangle = \sum_x a_x |x\rangle.$$

The coefficients a_x are called amplitudes and the sum of the squares of their modules is normalized:

$$\langle v|v\rangle = \sum_x |a_x|^2 = 1$$

The square of the magnitude of the amplitude a_x corresponds to the probability of observing the system in the classical state $|x\rangle$:

$$P[|x\rangle | |v\rangle] = |\langle x|v\rangle|^2 = \langle v| P_x |v\rangle, \quad (9)$$

where P_x is the projector onto the subspace $|x\rangle$.

When the state of a quantum system is uncertain, it is described as a statistical mixture of pure states, each occurring with a specified probability. This ensemble is referred to as a *mixed state*, which can be mathematically represented as:

$$\sum_v p_v |v\rangle, \quad \sum_v p_v = 1. \quad (10)$$

Here, p_v represents the probability of the system to be in the pure state $|v\rangle$, and the sum of all these probabilities is equal to 1.

The space of pure and mixed states forms a *convex* subspace within the Hilbert space \mathcal{H} . The extreme points of this subspace are the pure states, while the mixed states are considered as points within this convex subspace.

If the system is in the mixed state (10), then the expected value of an observable M from the ensemble is defined as:

$$\langle M \rangle = \sum_v p_v \langle v| M |v\rangle = \text{tr}(M\rho), \quad (11)$$

where ρ represents the *density matrix* or the *density operator* of the system:

$$\rho = \sum_v p_v \rho_v, \quad (12)$$

and ρ_v denotes the density operator of a pure state $|v\rangle$:

$$\rho_v = |v\rangle \langle v|.$$

The density operator encodes all the essential statistics of the ensemble even when the number of its pure states is greater than N . Formally, a density operator ρ is a bounded linear operator $\rho : \mathcal{H} \rightarrow \mathcal{H}$ with the following properties:

1. ρ is *Hermitian*, i.e. $\rho = \rho^\dagger$.
2. ρ is a non-negative definite: $\langle v | \rho | v \rangle \geq 0$, $\forall |v\rangle \in \mathcal{H}$.
3. ρ has unit trace: $\text{tr}(\rho) = 1$.
4. The eigenvalues $\lambda_1, \dots, \lambda_N$ of ρ form a probability distribution.

The density operators of pure states satisfy the equation $\rho = \rho^2$ and they form a complex projective space. In other words, they are projectors onto the one-dimensional subspaces of \mathcal{H} . We will denote the space of bounded linear operators on the Hilbert space \mathcal{H} by $B(\mathcal{H})$, the space of Hermitian operators by $H(\mathcal{H})$ and the space of corresponding density operators by $D(\mathcal{H})$. The space $H(\mathcal{H})$ is a linear vector space, but $D(\mathcal{H})$ is not. A general linear combination of density operators is Hermitian, but its trace is not necessarily equal to one. The space of density operators $D(\mathcal{H})$ forms an $N^2 - 1$ - dimensional convex space which embeds in $H(\mathcal{H})$ [49].

The classical Hidden Markov Models use linear operators to describe the stochastic evolution of states. Similarly, in the context of discrete-time quantum systems, quantum state transformations are defined by linear operators known as quantum operations. A quantum operation, denoted by \mathcal{O} , is a linear map:

$$\mathcal{O} : B(\mathcal{H}) \rightarrow B(\mathcal{H})$$

with the following properties:

1. \mathcal{O} preserves convex combinations of density operators. If the map is applied to a stochastic ensemble of density operators, then the outcome is the same ensemble of the resulting densities.
2. \mathcal{O} is trace preserving:

$$\text{tr}(\mathcal{O}\beta) = \text{tr}(\beta), \forall \beta \in B(\mathcal{H})$$

This property ensures the conservation of probability in physical processes.

3. \mathcal{O} is a *completely positive* map. It is positive: $\rho \geq 0 \rightarrow \mathcal{O}\rho \geq 0$, and it remains positive under any tensor product extensions. In other words, $(\mathcal{O} \otimes I_K)$ is positive for $\forall K > 0$.

These properties ensure that a quantum operation is a valid and consistent evolution of quantum states, preserving the probabilistic nature and positivity of density operators.

According to these properties a quantum operation is a *Completely Positive Trace-Preserving* (CPTP) linear map. It is commonly assumed that the evolution of a discrete-time quantum system can be described by a quantum operation. In the context of quantum communication, a quantum operation is often referred to as a *quantum channel*.

An example of quantum operation is the density operator evolution under unitary transformation U :

$$\mathcal{O}\rho = U\rho U^\dagger. \quad (13)$$

The general process of extracting classical information from a quantum state or *generalized measurement*, also can be described by quantum operation. The operation is a *complete* set of Hermitian non-negative operators $\mathcal{M} = \{E_e\}$ with decomposition $E_e = M_e^\dagger M_e$:

$$\mathcal{M}\rho = \sum_e M_e \rho M_e^\dagger. \quad (14)$$

The operators satisfy the *completeness* property $\sum_e E_e = I$ [24]. Each operator E_e is associated with a classical measurement outcome e . If the system is in an ensemble of pure states ρ each measurement outcome realizes with probability

$$P[e|\rho] = \text{tr}(E_e \rho). \quad (15)$$

The normalized state after observing outcome e is defined by

$$\rho_e = \frac{E_e \rho}{P[e|\rho]}. \quad (16)$$

A special case of generalized measurement is the *projective measurement*, where the Hermitian measurement operators $\{E_e\}$ in addition to satisfying the completeness property are orthogonal, i.e. $E_{e_1} E_{e_2} = \delta_{e_1, e_2} E_{e_1}$. In this case the operator \mathcal{M} has eigenstates $\{|e\rangle\}$ and eigenvalues $\{e\}$ which form an orthogonal basis in \mathcal{H} :

$$\mathcal{M} = \sum_e e E_e,$$

where $E_e = |e\rangle \langle e|$ are orthogonal projections on the corresponding eigenspaces. The outcome of the projective measurement corresponds to one of the eigenvalues $\{e\}$ associated with the measurement operators, and the post-measurement state of the system collapses to the corresponding eigenstate. In

contrast, for generalized measurement operations, the post-measurement states are mixed states, and the measurement outcomes are distributions of outcomes. Another important distinction between projective and generalized measurements is that the successive orthogonal measurements will produce the same outcome, while this is not the case for the generalized measurement operations.

The evolution of the hidden state is modeled by the dynamics of a quantum system with Hilbert space \mathcal{H}_S , dimension N and orthonormal basis $\{|s\rangle\}$. This quantum system represents the underlying dynamics of the stochastic process and is referred to as the "state" or S -system.

The emission process, which depends on the hidden state, is modeled by a second quantum system - *emission* system or E -system, with Hilbert space \mathcal{H}_E , dimension M , and orthonormal basis $\{|e\rangle\}$. The dimension M of the emission system is equal or greater than the number of the observable symbols of the stochastic process. To represent a quantum system composed of two subsystems, we use a quantum operation that combines the components through a tensor product, creating a *bipartite* quantum system:

$$\rho_S \mapsto \rho_S \otimes \rho_E = \rho_{SE}, \quad (17)$$

where the composed Hilbert space is

$$\mathcal{H}_{SE} = \mathcal{H}_S \otimes \mathcal{H}_E. \quad (18)$$

Here the state ρ_{SE} is a *tensor product state*, i.e. initially the subsystems are not entangled. A further

assumption is that the initial state of the emission component is a fixed pure state $\rho_E = |e_0\rangle\langle e_0|$, where $|e_0\rangle \in \{|e\rangle\}$.

In order to describe one of the components of a bipartite system while disregarding the other we use a quantum operation known as *partial trace* [24]. The partial trace operation is a linear transformation that maps the density operator of the bipartite system to the *reduced density* operator of one of the components:

$$\begin{aligned} \mathcal{O}\rho_{SE} &= \text{tr}_E(\rho_{SE}) \\ &= \text{tr}_E(\rho_S \otimes \rho_E) \\ &= \sum_e (I_N \otimes \langle e|) (\rho_S \otimes \rho_E) (I_N \otimes |e\rangle) \\ &= \rho_S \end{aligned} \quad (19)$$

The partial trace operation in (19) is applied to a non-entangled bipartite system and therefore the partial density of the state system is independent from the emission system.

To model joint stochastic processes a unitary operation (13) is applied to entangle the subsystems and transfer information from the hidden state to the observable:

$$\mathcal{O}_U\rho_{SE} = U\rho_{SE}U^\dagger.$$

The evolution of the hidden state is described by tracing out the emission component (19):

$$\begin{aligned} \text{tr}_E(\mathcal{O}_U\rho_{SE}) &= \text{tr}_E(U\rho_{SE}U^\dagger) = \text{tr}_E(U(\rho_S \otimes |e_0\rangle\langle e_0|)U^\dagger) \\ &= \sum_e I_N \otimes \langle e| [U((I_N \otimes |e_0\rangle\langle e_0|)\rho_S(I_N \otimes |e_0\rangle\langle e_0|))U^\dagger] I_N \otimes |e\rangle. \end{aligned} \quad (20)$$

The equation (20) defines *operator-sum representation* of the quantum operation \mathcal{T} as follows:

$$\mathcal{T}\rho_S = \sum_e K_e \rho_S K_e^\dagger. \quad (21)$$

where the operators $\{K_e\}$, known as *Kraus operators*, act on the state system ρ_S and are defined as follows:

$$K_e = (I^N \otimes \langle e|) U (I^N \otimes |e_0\rangle). \quad (22)$$

The Kraus operators depend on the unitary U , and the arbitrary selected orthonormal basis $\{|e\rangle\}$ of the

emission system. Since any unitary transformation of a basis is also an orthonormal basis, the operator-sum representation is defined up to a unitary transformation. A quantum operation can be represented by different number of Kraus operators but there is a minimum. The minimal integer r for which the operation \mathcal{T} has decomposition with r operators is called *Kraus rank* of the operation \mathcal{T} denoted by $\text{rank}(\mathcal{T})$. The Kraus rank is equal to the rank of a positive linear operator known as *Choi matrix* [50]

of the operation \mathcal{T} :

$$J_{\mathcal{T}} = \sum_{i,j=1}^N |i\rangle\langle j| \otimes \mathcal{T}(|i\rangle\langle j|). \quad (23)$$

The Kraus rank of a quantum operation ranges from 1 for unitary transformations to N^2 for completely depolarizing operations. Each Kraus operator has N^2 complex parameters, and all operators must satisfy the completeness constraint. Since the Kraus representation is unique up to a unitary transformation, the total number of free real parameters for a quantum operation is $N^4 - N^2$. The set of quantum operations is a convex set with extreme points defined by linearly independent Kraus operators $\{K_e\}$ with maximal rank N [50]. Every quantum operation can be represented as convex combination of N^2 extreme operations.

For every Kraus operator K_e we define a quantum operation T_e acting on the state ρ_S as follows:

$$T_e \rho_S = K_e \rho_S K_e^\dagger. \quad (24)$$

The operations $T_e = K_e^\dagger K_e$ are Hermitian and positive. They satisfy the completeness property $\sum_e T_e = I^N$, since the quantum operation \mathcal{T} defined in (21) is trace-preserving for all states ρ_S :

$$\text{tr}(\mathcal{T}\rho_S) = \text{tr}\left(\sum_e T_e \rho_S\right) = 1. \quad (25)$$

The operators $\{T_e\}$ define a generalized measurement or a *Positive Operator-Valued Measure* (POVM) operation on the state subsystem S . The probability distribution of the measurement outcomes is reflected in the post-measurement density operator $\mathcal{T}\rho_S$ (21). Each Kraus operator corresponds to a measurement outcome, and the set of Kraus operators forms a complete set of operators that span the space of possible measurement outcomes. Therefore, if the Kraus operators are linearly

independent, then the number of measurement outcomes is equal to the Kraus rank.

We have shown that when an entangled bipartite system is in a pure state, the states of its individual components exhibit characteristics similar to mixed states when observed independently or described using the partial trace operation. This property of the composite system is important as it allows the use of density operators as models of classical stochastic states, despite the underlying pure quantum nature of the system.

A mixed state of one of the components in an entangled bipartite pure state can also be defined by performing a projective measurement on the other component. The measurement outcome on one component provides information about the state of the other component due to the entanglement-related correlation between the components. Let $\{|e\rangle\}$ be an orthonormal basis of the emission component. The corresponding set of orthogonal projectors is:

$$\{M_e = |e\rangle\langle e|, e = 0, \dots, M-1\}.$$

We can extend this set to operators $\{P_e\}$ acting on the bipartite system:

$$P_e = I_N \otimes M_e.$$

The projective measurement operation on the full system is defined as (14):

$$\mathcal{M}(\rho_{SE}) = \sum_e P_e \rho_{SE} P_e^\dagger.$$

The measurement outcomes have probabilities defined in (15):

$$P[e | U\rho_{SE}U^\dagger] = \text{tr}(P_e U(\rho_S \otimes \rho_E)U^\dagger P_e^\dagger).$$

These probabilities depend on the Kraus operators defined in (22), and can be expressed in terms of the measurement basis $\{|e\rangle\}$:

$$\begin{aligned} P[e | U\rho_{SE}U^\dagger] &= \text{tr}(P_e U(\rho_S \otimes \rho_E)U^\dagger P_e^\dagger) \\ &= \text{tr}(I_N \otimes \langle e| [U((I_N \otimes |e_0\rangle)\rho_S(I_N \otimes \langle e_0|))U^\dagger] I_N \otimes |e\rangle) \\ &= \text{tr}(K_e \rho_S K_e^\dagger) \\ &= \text{tr}(T_e \rho_S) \end{aligned} \quad (26)$$

We can summarize that in a bipartite system $\rho_{SE} = \rho_S \otimes \rho_E$ the operation of entanglement of the components, followed by tracing out of one com-

ponent, e.g. ρ_E , has the same operator-sum representation as a projective measurement of ρ_E and "discarding" the outcome. Both cases are equivalent

to a POVM operation on ρ_S as defined in (24):

$$\begin{aligned} \mathcal{T}\rho_S &= \sum_e (P_e U (\rho_S \otimes \rho_E) U^\dagger P_e^\dagger) \\ &= \sum_e K_e \rho_S K_e^\dagger = \sum_e T_e \rho_S \quad (27) \\ &= \mathcal{M}\rho_S. \end{aligned}$$

The equality in (27) provides two equivalent approaches for modeling the joint process of a state evolution and dependent symbol emission. It can be represented either as a POVM operation on the state system or as a unitary transformation U entangling the full system followed by a projective measurement on the emission component. In both cases, the state of the state system S becomes a mixed state, representing a stochastic ensemble that averages all possible post-measurement states. This behavior reflects the characteristics of classical stochastic generators and allows the quantum model to reflect the probabilistic nature of the joint stochastic process.

III. QUANTUM HIDDEN MARKOV MODELS

The POVM operations (24) as described in Section II B define a joint stochastic process of quantum state transitions and symbols emission. The quantum operation acting on a quantum state resembles the classical observable operators (3) transforming a classical stochastic state as defined in Section II A. These similarities provide the foundation for the following quantum hidden Markov model (QHMM) definition.

Definition 2 (Quantum Hidden Markov Model [25]). *A quantum HMM (QHMM) \mathbf{Q} over an N -dimensional Hilbert space \mathcal{H} is a 4-tuple:*

$$\mathbf{Q} = \{\Sigma, \mathcal{H}, \mathcal{T} = \{T_a\}_{a \in \Sigma}, \rho_0\}, \quad (28)$$

where

- Σ is a finite alphabet of observable symbols.
- \mathcal{H} is an N -dimensional Hilbert space with space of density operators $D(\mathcal{H})$.
- \mathcal{T} is a CPTP map (quantum channel) $\mathcal{T} : D(\mathcal{H}) \rightarrow D(\mathcal{H})$.
- $\{T_a\}_{a \in \Sigma}, \sum_{a \in \Sigma} T_a^\dagger T_a = I_N$ is an operator-sum representation of \mathcal{T} in terms of a complete set of Kraus operators.
- ρ_0 is an initial state, $\rho_0 \in D(\mathcal{H})$.

When the operation $\mathcal{T} = \{T_a\}_{a \in \Sigma}$ is applied to the state $\rho \in D(\mathcal{H})$, any symbol $a \in \Sigma$ will be observed/emitted with probability (15):

$$P[a|\rho] = \text{tr}(T_a \rho)$$

and the system's state will become (16):

$$\rho_a = \frac{T_a \rho}{P[a|\rho]}.$$

If the operation \mathcal{T} is applied t times starting at the initial state the model will emit a sequence of symbols $\mathbf{a} = a_1 \dots a_t$ with probability

$$P[\mathbf{a}|\rho_0] = \text{tr}(T_{\mathbf{a}} \rho_0). \quad (29)$$

where

$$T_{\mathbf{a}} = T_{a_t} \dots T_{a_1} \quad (30)$$

For each QHMM \mathbf{Q} the equation (29) defines a *sequence function* $f^{\mathbf{Q}}$ and corresponding Hankel matrix (7) $H^{\mathbf{Q}}$ as follows:

$$f^{\mathbf{Q}}(\mathbf{a}) = P[\mathbf{a}|\rho_0], \forall \mathbf{a} \in \Sigma^*, \quad (31)$$

$$H^{\mathbf{Q}}[\mathbf{p}, \mathbf{s}] = f^{\mathbf{Q}}(\mathbf{ps}), \forall \mathbf{p}, \mathbf{s} \in \Sigma^*. \quad (32)$$

The sequence function (31) defines a distribution $D_t^{\mathbf{Q}}$ over the sequences of length t for $\forall t > 0$:

$$D_t^{\mathbf{Q}} = \{f^{\mathbf{Q}}(\mathbf{a}) : \mathbf{a} \in \Sigma^t\} \quad (33)$$

Therefore, every QHMM \mathbf{Q} defines a *stochastic process language* $\mathbf{L}^{\mathbf{Q}}$ (1) over the set of finite sequences Σ^* .

The eigenvector ρ^* of the quantum operation \mathcal{T} with eigenvalue 1, normalized to represent a distribution, is the *steady state* of the model \mathbf{Q} :

$$\rho^* = \mathcal{T}\rho^*. \quad (34)$$

The dimension of the Hilbert space $\dim(\mathcal{H}) = N$ is called *order* of the quantum model \mathbf{Q} .

Any iteration of the quantum operation \mathcal{T} :

$$\rho_t = \mathcal{T}^t \rho_0, t \geq 0, \quad (35)$$

defines a mixed state ρ_t , which corresponds to all the stochastic paths for generation of a symbol sequence with length t .

The following theorem, presented in [25], shows that QHMMs can generate the class of languages generated by the classic HMMs.

Theorem 2 (Monras [25]). *For every classic HMM of order N there exists a QHMM of the same order which generates the same stochastic process language.*

The proof is by construction of a QHMM \mathbf{Q} equivalent to any given classic HMM. Let's consider a classic HMM \mathbf{C} , defined by alphabet Σ of m observable symbols, space of n unobservable (hidden) process states, initial state distribution \mathbf{x}_0 and a set of observable operators $\mathbf{O} = \{O_a | a \in \Sigma\}$ as defined in (3). We can define an equivalent (generating the same stochastic language) QHMM \mathbf{Q} with Hilbert space \mathcal{H} with dimension $N = n$ as follows:

$$\mathbf{Q} = \{\Sigma, \mathcal{H}, \mathcal{T} = \{T_a\}_{a \in \Sigma}, \rho_0\},$$

where

1. The initial density operator is $\rho_0 = |0\rangle\langle 0|$.
2. Model's states are the diagonal density operators:

$$D(\mathcal{H}) : \{\rho_i = |i\rangle\langle i| | i \in [0, N-1]\}.$$
3. The components of the quantum operation \mathcal{T} are defined as

$$T_a = \sum_{ij} K_a^{ij} K_a^{ij\dagger} \quad (36)$$

where

$$K_a^{ij} = \sqrt{O_a[i, j]} |i\rangle\langle j|.$$

We can verify using (36), (4), and (29), that for every sequence $\mathbf{a} \in \Sigma^*$ the classical and quantum HMMs define equal probability:

$$P[\mathbf{a} | \mathbf{C}, s_0] = \mathbf{1}_{\mathbf{O}_a \mathbf{x}_0} = \text{tr}(T_{a_1} \dots T_{a_n} \rho_0) = P[\mathbf{a} | \mathbf{Q}, \rho_0]$$

and therefore they define the same stochastic language.

The QHMM construction above simulates a classic HMM of order n in a Hilbert space with dimension $N = n$. It is important to find out whether the quantum framework allows more efficient representation of the stochastic process languages.

Let's assume that a classical HMM \mathbf{M} and a QHMM \mathbf{Q} define the same stochastic process language L . If H^L is the generalized Hankel matrix (7) associated with L , then it is proven [20] that $\text{rank}(H^L)$ provides lower bound of the order of the classic models defining L . The bound can be reached for the classic HMM, i.e. if the stochastic language is defined by a classic HMM, then there exists minimal classic HMM defining L with exactly $\text{rank}(H^L)$ states. In order to prove similar statements for the QHMM, since the states are represented by density operators, it is necessary to estimate the size of a basis consisting of orthonormal density operators. The space of density operators $D(\mathcal{H})$ is a closed and

bounded convex space with dimension $N^2 - 1$. The extreme point of $D(\mathcal{H})$ are the density operators of the pure states. Extensive study of the geometry of $D(\mathcal{H})$ is presented for example in [49]. Here we will show that the space of Hermitian matrices $H(\mathcal{H})$ is spanned by a set of N^2 density operators. We will prove the following proposition.

Proposition 1. *For any Hilbert space \mathcal{H} with dimension N there is a basis of density operators $B_D \subset D(\mathcal{H})$ with size N^2 which spans the space of Hermitian operators $H(\mathcal{H})$.*

Proof. The computational basis for a Hilbert space \mathcal{H} with dimension N consists of N orthonormal vectors:

$$\{|i\rangle : \langle i|j\rangle = \delta_{ij}, i \in [0, N-1], j \in [0, N-1]\}$$

We will define the basis set B_H of Hermitian operators as follows:

$$\begin{aligned} B_H = & \{|i\rangle\langle i| : i \in [0, N-1]\} \cup \\ & \{|i\rangle\langle j| + |j\rangle\langle i| : 0 \leq i < j \leq N-1\} \cup \\ & \{i(|i\rangle\langle j| - |j\rangle\langle i|) : 0 \leq i < j \leq N-1\}, \end{aligned}$$

where i is the imaginary unit.

It is easy to verify that the set B_H contains $N^2 = N + \binom{N}{2} + \binom{N}{2}$ linearly independent operators which span the space $H(\mathcal{H})$. The set contains three groups of Hermitian operators. The first group contains diagonal operators, projectors onto each computational basis state $|i\rangle$. The second group contains symmetric operators representing the off-diagonal components of Hermitian matrices. The third group contains antisymmetric operators representing the imaginary off-diagonal parts of Hermitian matrices.

We will define a basis of density operators B_D which span $H(\mathcal{H})$ by transforming the elements of B_H (which are not density operators) to density operators using operation of element-wise summation and real scalar multiplication. These operations will change the Hermitian basis B_H to a density basis B_D as follows:

- The set of diagonal operators $|i\rangle\langle i|$ which are density operators will not be changed.

$$\{|i\rangle\langle i| : i \in [0, N-1]\}$$

- Each non-diagonal symmetric operator $|i\rangle\langle j| + |j\rangle\langle i|$ is traceless. To ensure that the resulting operator has a unit trace, we sum it with the corresponding diagonal operators and normalize the trace multiplying by the real scalar $\frac{1}{2}$:

$$\frac{1}{2}(|i\rangle\langle j| + |j\rangle\langle i| + |i\rangle\langle i| + |j\rangle\langle j|)$$

These operators are symmetric with unit trace, and they are positive semi-definite because they can be directly expressed as scaled outer products $\frac{1}{2} |v\rangle \langle v|$, where $|v\rangle$ is a linear combination of computational basis vectors:

$$|v\rangle = |i\rangle + |j\rangle$$

Therefore they are density operators.

- Each non-diagonal anti-symmetric operator $i(|i\rangle \langle j| - |j\rangle \langle i|)$ is traceless and we also sum it with the corresponding diagonal operators and normalize the trace multiplying by the real scalar $\frac{1}{2}$:

$$\frac{1}{2}(i(|i\rangle \langle j| - |j\rangle \langle i|) + |i\rangle \langle i| + |j\rangle \langle j|)$$

These operators are anti-symmetric with unit trace, and they are positive semi-definite because they can be directly expressed as scaled outer products $\frac{1}{2} |v\rangle \langle v|$, where $|v\rangle$ is linear combination of computational basis vectors:

$$|v\rangle = i|i\rangle - |j\rangle$$

These operators are density operators.

The derived set of density operators then becomes:

$$\begin{aligned} B_D = & \{|i\rangle \langle i| : 0 \leq i \leq N-1\} \cup \\ & \left\{ \frac{1}{2} (|i\rangle \langle j| + |j\rangle \langle i| + |i\rangle \langle i| + |j\rangle \langle j|) \right\} \cup \\ & \left\{ \frac{1}{2} (i(|i\rangle \langle j| - |j\rangle \langle i|) + |i\rangle \langle i| + |j\rangle \langle j|) \right\}, \\ & 0 \leq i < j \leq N-1 \end{aligned} \quad (37)$$

The operators in B_D are linearly independent because:

1. The density operators are linearly independence within each group (diagonal, symmetric, and anti-symmetric) because they act on distinct pairs of basis vectors $|i\rangle, |j\rangle$.
2. The density operators belonging to different groups are linearly independent because they act on distinct subspaces of the Hilbert space:
 - The diagonal operators $|i\rangle \langle i|$ act only on the diagonal elements of the matrix.
 - The symmetric and anti-symmetric operators act on both the diagonal and off-diagonal elements.
 - The symmetric operators are real, while the anti-symmetric operators always have imaginary component. A real operator cannot be written as a linear combination of operators with imaginary components using real scalars.

Since the set B_D contains N^2 linearly independent density operators it spans the space of Hermitian operators with dimension N^2 . \square

The existence of a set of linearly independent density operators with size N^2 that span the space $\mathcal{H}(\mathcal{H})$ allows to estimate an upper bound on the rank of the stochastic process languages described by QHMMs. The following theorem provides a necessary condition for a finite-rank stochastic language to be generated by a QHMM.

Theorem 3. *Let H be the infinite Hankel matrix associated with a quantum hidden Markov model (QHMM) \mathbf{Q} of order N . Then:*

$$\text{rank}(H) \leq N^2.$$

Proof. Consider a QHMM \mathbf{Q} as defined in (28), and let $B_D = \{b_m\}_{m=1}^{N^2}$ be a basis of the Hermitian operator space $\mathcal{H}(\mathcal{H})$, consisting of density operators $b_m \in D(\mathcal{H})$ as established in **Proposition 1**.

For each operator $b_m \in B_D$, define the sequence function $f_m : \Sigma^* \rightarrow \mathbb{R}$ as:

$$f_m(\mathbf{a}) = \text{tr}(T_{a_t} \cdots T_{a_1} b_m), \quad \forall \mathbf{a} \in \Sigma^t, t \geq 0. \quad (38)$$

We will show that the functions $\{f_m\}$ generate the column space of the Hankel matrix H . For any prefix and suffix sequences:

$$\mathbf{p} = p_1 \cdots p_r, \quad \mathbf{s} = s_1 \cdots s_t,$$

the entries of the Hankel matrix H are defined by (29):

$$\begin{aligned} H[\mathbf{p}, \mathbf{s}] &= \text{tr}(T_{s_t} \cdots T_{s_1} T_{p_r} \cdots T_{p_1} \rho_0) \\ &= \text{tr}(T_{s_t} \cdots T_{s_1} \rho_{\mathbf{p}}), \end{aligned}$$

where we define the density operator:

$$\rho_{\mathbf{p}} = T_{p_r} \cdots T_{p_1} \rho_0.$$

Since $\rho_{\mathbf{p}} \in \mathcal{H}(\mathcal{H})$, it can be expressed in the basis B_D :

$$\rho_{\mathbf{p}} = \sum_{m=1}^{N^2} c_{\mathbf{p},m} b_m,$$

for some coefficients $c_{\mathbf{p},m} \in \mathbb{R}$.

Substituting this decomposition into the expression for $H[\mathbf{p}, \mathbf{s}]$:

$$\begin{aligned} H[\mathbf{p}, \mathbf{s}] &= \text{tr} \left(T_{s_t} \cdots T_{s_1} \sum_{m=1}^{N^2} c_{\mathbf{p},m} b_m \right) \\ &= \sum_{m=1}^{N^2} c_{\mathbf{p},m} \text{tr}(T_{s_t} \cdots T_{s_1} b_m) \\ &= \sum_{m=1}^{N^2} c_{\mathbf{p},m} f_m(\mathbf{s}). \end{aligned} \quad (39)$$

Now, consider the row vector of H corresponding to prefix \mathbf{p} :

$$R_{\mathbf{p}} = H[\mathbf{p}, \cdot].$$

From (39), we have:

$$R_{\mathbf{p}}(\mathbf{s}) = \sum_{m=1}^{N^2} c_{\mathbf{p},m} f_m(\mathbf{s}).$$

Thus, each row of the Hankel matrix is a linear combination of the sequence functions f_m , demonstrating that the set $\{f_m\}_{m=1}^{N^2}$ spans the row space of H .

This representation allows us to factorize the Hankel matrix H as:

$$H = CF, \quad (40)$$

where:

$$C[\mathbf{p}, m] = c_{\mathbf{p},m}, \mathbf{p} \in \Sigma^*, m \in [1, \dots, N^2],$$

$$F[m, \mathbf{s}] = f_m(\mathbf{s}), \mathbf{s} \in \Sigma^*, m \in [1, \dots, N^2],$$

Substituting into (40):

$$H[\mathbf{p}, \mathbf{s}] = \sum_{m=1}^{N^2} c_{\mathbf{p},m} f_m(\mathbf{s}).$$

Since H is expressed as the product of a $(\infty \times N^2)$ matrix C and an $(N^2 \times \infty)$ matrix F , the rank of H is bounded by:

$$\text{rank}(H) \leq N^2. \quad \square$$

A comparison of **Theorem 1** and **Theorem 3** shows that quantum models provide compact representation of the stochastic languages. They require a quadratically smaller state space to generate a finite-rank language compared to their classical counterparts.

Next, we provide a sufficient condition, guaranteeing that for any stochastic language of finite rank, there exists a QHMM that generates it. We also establish the explicit Hilbert space dimension required to construct such a QHMM.

Theorem 4. *For every stochastic language of finite rank r over an alphabet of m symbols, there exists a quantum hidden Markov model (QHMM) \mathbf{Q} , defined in a Hilbert space of dimension*

$$N = \left\lceil \left(0.5 + \sqrt{0.25 + mr^2} \right)^{\frac{1}{2}} \right\rceil,$$

that generates the given stochastic language.

Proof. Let L be a finite-rank stochastic process language with an associated Hankel matrix H of finite rank r . To construct a finite representation of H , select r linearly independent rows, indexed by their corresponding prefixes in the Hankel matrix. Denote this set of prefixes as:

$$P = \{\mathbf{p}_1, \dots, \mathbf{p}_r\}.$$

Since the rows in P form a basis for the row space of H , the row corresponding to any prefix \mathbf{p} can be expressed as a linear combination of the basis rows. That is, there exist coefficients $\alpha_1, \dots, \alpha_r \in \mathbb{R}$ such that:

$$H[\mathbf{p}, \cdot] = \sum_{i=1}^r \alpha_i H[\mathbf{p}_i, \cdot]. \quad (41)$$

Assume that the process is in state q_i , represented by the basis prefix \mathbf{p}_i . Upon emitting a symbol a , the process transitions to a new state defined by the concatenated prefix $\mathbf{p}_i a$. The conditional observation probabilities are defined by the Hankel matrix:

$$\begin{aligned} P[a|q_i] &= \frac{P[\mathbf{p}_i a]}{P[\mathbf{p}_i]} \\ &= \frac{H[\mathbf{p}_i a, \epsilon]}{H[\mathbf{p}_i, \epsilon]} \end{aligned} \quad (42)$$

By the linear structure of the language established in (41), the row of the Hankel matrix indexed by $\mathbf{p}_i a$ can be expressed as:

$$H[\mathbf{p}_i a, \cdot] = \sum_{j=1}^r \alpha_{i,j}^{(a)} H[\mathbf{p}_j, \cdot], \quad (43)$$

where $\alpha_{i,j}^{(a)} \in \mathbb{R}$ are the linear coefficients that describe how the new row is represented as a linear combination of the basis rows in P .

This linear structure is directly reflected in the relation between the corresponding sequence probabilities. In particular:

$$P[\mathbf{p}_i a] = \sum_{j=1}^r \alpha_{i,j}^{(a)} P[\mathbf{p}_j]. \quad (44)$$

Here, $P[\mathbf{p}_i a]$ denotes the probability of observing the sequence defined by the prefix \mathbf{p}_i followed by the symbol a , while $P[\mathbf{p}_j]$ correspond to the probabilities associated with the basis prefixes. According to equation (44), the probability of any observed sequence can be expressed as a linear combination of the probabilities of the basis prefixes.

Substituting (44) into the classical conditional probability formula (42) yields:

$$P[a | \mathbf{p}_i] = \frac{\sum_{j=1}^r \alpha_{i,j}^{(a)} P[\mathbf{p}_j]}{P[\mathbf{p}_i]}. \quad (45)$$

The non-normalized conditional transition probabilities allocated to the states q_j are :

$$P[q_j|q_i, a] = \alpha_{i,j}^{(a)} P[\mathbf{p}_j], \quad j = 1, \dots, r \quad (46)$$

These probabilities represent the contributions from states q_j when transitioning from q_i on symbol a .

From (46) we define the state transition matrix $\tau^{(a)}$ for each observable symbol $a \in \Sigma$:

$$\tau_{i,j}^{(a)} = P[q_j|q_i, a], \quad j = 1, \dots, r \quad (47)$$

The initial state distribution $\omega \in \mathbb{R}^r$ is a stochastic vector and depends on $r - 1$ free parameters. These parameters can be determined from the linear system:

$$\mathbf{1}^\top \tau^{\mathbf{p}_i} \omega = H[\mathbf{p}_i, \epsilon], \quad i = 1, \dots, r - 1, \quad (48)$$

where $\mathbf{1} = (1, \dots, 1)^\top \in \mathbb{R}^r$ is the all-ones vector, and:

$$\tau^{\mathbf{p}_i} = \prod_{j=k}^1 \tau^{a_j}, \quad \mathbf{p}_i = a_1 \dots a_k.$$

Equation (48) ensures that the initial state distribution is consistent with the given Hankel matrix probabilities for the selected basis prefixes.

Consider a QHMM \mathbf{Q} defined in a Hilbert space \mathcal{H} of dimension N as per Definition (2). By **Proposition 1**, there exists a basis of density operators spanning the space $\mathcal{H}(\mathcal{H})$ with size N^2 :

$$B = \{b_1, \dots, b_{N^2}\}. \quad (49)$$

Any state $\rho \in D(\mathcal{H})$ of the QHMM can be expressed as a linear combination of the basis elements:

$$\rho = \sum_{i=1}^{N^2} d_i^{(\rho)} b_i,$$

where $d_i^{(\rho)} \in \mathbb{R}$ are real expansion coefficients that depend on ρ .

Let K_a be the Kraus operator corresponding to the emission of symbol $a \in \Sigma$. The updated state after observing a is:

$$\begin{aligned} \rho^{(a)} &= K_a \rho K_a^\dagger \\ &= K_a \left(\sum_{i=1}^{N^2} d_i^{(\rho)} b_i \right) K_a^\dagger \\ &= \sum_{i=1}^{N^2} d_i^{(\rho)} (K_a b_i K_a^\dagger). \end{aligned} \quad (50)$$

This shows that the action of K_a on a superposition of basis states is the corresponding superposition of the transformed basis elements:

$$b_i^{(a)} := K_a b_i K_a^\dagger. \quad (51)$$

The probability of observing symbol a given that the system is in basis state b_i is:

$$P[a | b_i] = \text{tr}(b_i^{(a)}). \quad (52)$$

Since each transformed basis element $b_i^{(a)}$ can be expanded back into the original basis B :

$$b_i^{(a)} = \sum_{j=1}^{N^2} \gamma_{i,j}^{(a)} b_j, \quad (53)$$

where $\gamma_{i,j}^{(a)} \in \mathbb{R}$ are expansion coefficients depending on both K_a and the structure of the basis B . Substituting (53) into (52) yields:

$$\begin{aligned} P[a | b_i] &= \text{tr} \left(\sum_{j=1}^{N^2} \gamma_{i,j}^{(a)} b_j \right) \\ &= \sum_{j=1}^{N^2} \gamma_{i,j}^{(a)} \text{tr}(b_j) \\ &= \sum_{j=1}^{N^2} P[b_j | b_i, a], \end{aligned} \quad (54)$$

where $\text{tr}(b_j) = 1$ and

$$P[b_j | b_i, a] = \gamma_{i,j}^{(a)} \quad (55)$$

represents the unnormalized local probability mass allocated to state b_j when transitioning from b_i upon emitting symbol a . The coefficients $\gamma_{i,j}^{(a)}$ quantify how the probability mass is distributed across basis states after applying the Kraus operator. Since the basis B is generally non-orthogonal, the expansion coefficients $\gamma_{i,j}^{(a)}$ may be negative even though $b_i^{(a)}$ is positive semidefinite. The coefficients $\gamma_{i,j}^{(a)}$ act as local expansion weights and do not individually guarantee positivity. The overall positivity is ensured at the operator level rather than at the coefficient level.

This phenomenon parallels the classical model's expansion coefficients $\alpha_{i,j}^{(a)}$ in (44), which can also take negative values despite the underlying process being probabilistic.

To account for the non-orthogonality of the basis, define the Gram matrix $G \in \mathbb{R}^{N^2 \times N^2}$ with entries:

$$G_{jk} = \text{tr}(b_j b_k).$$

Then, the expansion coefficients can be explicitly expressed as:

$$\gamma_{i,j}^{(a)} = \sum_{k=1}^{N^2} (G^{-1})_{jk} \text{tr}(b_k K_a b_i K_a^\dagger). \quad (56)$$

To ensure that the QHMM \mathbf{Q} accurately simulates the classical stochastic process defined by (46), it is essential to establish a relationship between the transition probabilities in both models. The equality of non-normalized conditional transition probabilities allocated to the basis classical states q_j (46) and quantum states b_i (55) establish relation between the coefficients $\alpha_{i,j}^{(a)}$ and $\gamma_{i,j}^{(a)}$:

$$\alpha_{i,j}^{(a)} = \frac{\gamma_{i,j}^{(a)}}{P[\mathbf{p}_j]} \quad (57)$$

This equality enables the construction of Kraus operators that reproduce the probabilistic transitions of the classical stochastic language. In particular, the expansion coefficients $\gamma_{i,j}^{(a)}$ (56) are quadratic functions of the parameters of the Kraus operators K_a .

For a finite-rank r stochastic language with m observable symbols $\{a_1, \dots, a_m\}$, the classical process defines mr^2 parameters $\alpha_{i,j}^{(a)}$, corresponding to m transition matrices (47). The probabilities of the basis prefixes \mathbf{p}_j are defined by the Hankel matrix.

In the quantum case, each Kraus operator K_a acts on an N -dimensional Hilbert space. A quantum system of dimension N can accommodate up to $N^4 - N^2$ real parameters through its Kraus operators. To ensure the existence of a solution for the system of quadratic equations, we require:

$$N \geq \left\lceil \left(0.5 + \sqrt{0.25 + mr^2} \right)^{\frac{1}{2}} \right\rceil. \quad (58)$$

Under this condition, the number of parameters available from the Kraus operators exceeds the number of equations defining the classical transition structure. The relationship between the Kraus parameters and the classical transition coefficients is given by (56):

$$\sum_{k=1}^{N^2} (G^{-1})_{jk} \text{tr}(b_k K_a b_i K_a^\dagger) = \alpha_{i,j}^{(a)} P[\mathbf{p}_j]. \quad (59)$$

Since the system is underdetermined (given the dimension condition (58)), solutions always exist in the complex field \mathbb{C} due to the algebraic closure property.

The final step is to define the initial state ρ_0 of the quantum model. It depends on $N^2 - 1$ real parameters. These parameters are determined by the system of equations derived from the Hankel matrix:

$$\text{tr}(T_{\mathbf{p}} \rho_0) = H[\mathbf{p}, \epsilon], \quad \mathbf{p} \in P, \quad (60)$$

where P is the basis set of r linearly independent prefixes. There are r equations and $N^2 - 1$ variables. Using the estimate (58) we have

$$N^2 - 1 \geq \left\lceil \left(-0.5 + \sqrt{0.25 + mr^2} \right) \right\rceil. \quad (61)$$

For every $m > 1$ the inequality (61) implies

$$N^2 - 1 \geq r. \quad (62)$$

Therefore, under the condition (58) there exists a QHMM that reproduces the classical stochastic process characterized by the finite-rank Hankel matrix H . \square

The theorem demonstrates a fundamental distinction between quantum stochastic generative models and classical hidden Markov models (HMMs). While a finite Hankel rank is a necessary condition for an HMM representation, it is not sufficient [41, 42, 44, 51]. In contrast, Theorem 4 asserts that every finite-rank stochastic process language can be generated by a quantum stochastic generator as a quantum hidden Markov model (QHMM). This implies that while every classical HMM can be embedded within a QHMM, there exist stochastic processes that admit QHMM representations but lack classical HMM representations. Consequently, the class of languages generated by QHMMs is a proper superset of those generated by classical HMMs.

A. Unitary Definition of QHMM

The definition of a QHMM in the previous section is based on the concept of a POVM operation acting on a quantum state. The emission of the observable symbols is encoded in the operational elements (Kraus operators) of the quantum operation. This framework provides a convenient way to view QHMMs as channels for quantum information processing. It allows for the analysis of their informational complexity, expressive capacity, and establishes connections to stochastic process languages and the corresponding automata. However, this approach cannot be directly used for the implementation of the QHMMs on quantum computing hardware.

In Section IIB we demonstrated that every POVM operation \mathcal{T} defined in Hilbert space \mathcal{H}_S can be represented as composition of basic quantum operations:

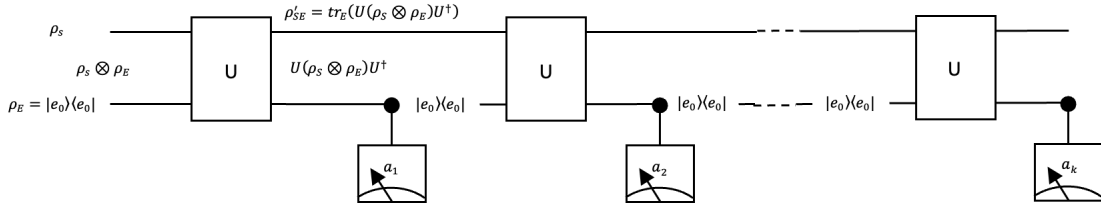


FIG. 2. Unitary Simulation of a Quantum Operation.

1. Dilation of the “state” system with an “emission” quantum system \mathcal{H}_E :

$$\mathcal{H}_S \mapsto \mathcal{H}_S \otimes \mathcal{H}_E.$$

2. Unitary transformation U , entangling the components of the bipartite system ρ_{SE} :

$$U(\rho_S \otimes \rho_E)U^\dagger.$$

3. Partial trace over the emission component, which provides the reduced density of the state system as the output of the operation:

$$\rho_S = \text{tr}_E (U(\rho_S \otimes \rho_E)U^\dagger).$$

The minimal dimension of the emission system \mathcal{H}_E corresponds to the Kraus rank of the operation \mathcal{T} . This rank quantifies the operation’s complexity by indicating the minimal auxiliary resources required for its unitary implementation. The unitary implementation of a QHMM relies on Stinespring’s dilation theorem [39], which states that any quantum operation can be represented as a unitary evolution on a larger (dilated) system.

Theorem 5. Any QHMM $\mathbf{Q} = \{\Sigma, \mathcal{H}_S, \mathcal{T} = \{T_a\}_{a \in \Sigma}, \rho_0\}$ has parameterization in terms of a unitary U defined in a dilated Hilbert space \mathcal{H} , where $\dim \mathcal{H} \geq \dim \mathcal{H}_S + |\Sigma|$.

Proof. Let’s introduce an auxiliary (“emission”) quantum system with Hilbert space \mathcal{H}_E , $\dim(\mathcal{H}_E) = M$, $M = |\Sigma|$, and orthonormal basis $\{|e_i\rangle\}_{i=0}^{M-1}$. We assume that $\text{ord}(a)$ is the position of the symbol a in the set $\Sigma = \{a_1, \dots, a_{M-1}\}$. Let’s select a specific state $|e_0\rangle$ to be the initial state. A linear operator $V : \mathcal{H}_S \rightarrow \mathcal{H}_S \otimes \mathcal{H}_E$ is defined as follows:

$$V : |v\rangle \mapsto \sum_{a \in \Sigma} T_a |v\rangle \otimes |e_{\text{ord}(a)}\rangle, |v\rangle \in \mathcal{H}_S. \quad (63)$$

Since the quantum operation \mathcal{T} is complete: $\sum_{a \in \Sigma} T_a^\dagger T_a = I_N$, the operator V is an isometry: $V^\dagger V = I_N$, and it can be extended to a unitary

operator $U : \mathcal{H}_S \otimes \mathcal{H}_E \rightarrow \mathcal{H}_S \otimes \mathcal{H}_E$ by using the Gram-Schmidt process [24].

If we apply the unitary operator U to the dilated system $\mathcal{H}_S \otimes \mathcal{H}_E$ and trace over the emission sub-system

$$\text{tr}_E (U(|v\rangle \langle v| \otimes |e_0\rangle \langle e_0|)U^\dagger) = \sum_{a \in \Sigma} T_a |v\rangle \langle v| T_a^\dagger,$$

where $|v\rangle \in \mathcal{H}_S$, we derive the operator-sum representation of \mathbf{Q} . Hence, the unitary U parameterizes the QHMM. \square

The above parameterization is unique up to a unitary transformation on the selected basis of the emission system.

Every unitary operator U acting on a composite system $\mathcal{H}_{SE} = \mathcal{H}_S \otimes \mathcal{H}_E$ defines a quantum operation by the Kraus operators (22). Every quantum operation defines a unitary operator on a dilated system through the isometry V (63). This equivalence allows us to provide a formal definition of unitary QHMMs.

Definition 3 (Unitary Quantum Hidden Markov Model). A Unitary Quantum HMM \mathbf{Q} over an alphabet of observable symbols Σ and finite N -dimensional Hilbert space is a 6-tuple:

$$\mathbf{Q} = \{\Sigma, \mathcal{H}_S, \mathcal{H}_E, U, \mathcal{M}, R_0\}$$

where

- Σ is a finite set of m observable symbols.
- \mathcal{H}_S is the Hilbert space of the hidden state system of dimension N .
- \mathcal{H}_E is the Hilbert space of an auxiliary emission system with dimension $m \leq M \leq N^2$ and orthonormal basis $E = \{|e_i\rangle\}_{i=0}^{M-1}$.
- U is a unitary operator defined on the bipartite Hilbert space $\mathcal{H}_S \otimes \mathcal{H}_E$.
- \mathcal{M} is a bijective map $\mathcal{P}_m^E \rightarrow \Sigma$, where \mathcal{P}_m^E is an m -element partition of E .

- $R_0 = \rho_0 \otimes |e_0\rangle\langle e_0|$ is an initial state.

The Algorithm 1 simulates a unitary QHMM \mathbf{Q} for T steps and generates a sequence of the process language $L^{\mathbf{Q}}$. The same generation process is presented graphically on FIG 2.

Algorithm 1: QHMM Unitary Simulation

Input : QHMM

$$\mathbf{Q} = \{\Sigma, \mathcal{H}_S, \mathcal{H}_E, U, \mathcal{M}, R_0 = \rho_0 \otimes |e_0\rangle\langle e_0|\}$$

Output: Generated Sequence \mathbf{a}

1 **Initialize:**

- **State system**
 $\mathcal{H}_S, \dim(\mathcal{H}_S) = N, \rho_S = \rho_0$
- **Emission system** $\mathcal{H}_E, \dim(\mathcal{H}_E) = M, m \leq M \leq N^2, \rho_E = |e_0\rangle\langle e_0|$
- **Prepare product state**
 $\rho_{SE} = \rho_S \otimes \rho_E$
- **Sequence length:** T
- **Current Step:** $t \leftarrow 0$
- **Output Sequence:** $\mathbf{a} \leftarrow \epsilon$

2 **while** $t \leq T$ **do**

```

3    $\rho_{SE} \leftarrow U \rho_{SE} U^\dagger$  /* Apply unitary on
   full system */
4    $\rho_S \leftarrow \text{tr}_E(\rho_{SE})$  /* Projective
   measurement of  $\rho_E$  */
5    $o \leftarrow e_i$  /* Measurement outcome  $o$  */
6    $\mathbf{a} \leftarrow \mathbf{a} + \mathcal{M}(E_o), E_o \in \mathcal{P}_m^E, o \in E_o$ 
   /* Emit symbol for outcome  $o$  */
7    $\rho_{SE} \leftarrow \rho_S \otimes |e_0\rangle\langle e_0|$  /* Set  $\rho_E$  to
   initial state */
8    $t \leftarrow t + 1$ 

```

9 **return** \mathbf{a}

Example 2. In [25], Monras et al. discuss an example of QHMM in Hilbert space with dimension 2, which defines a stochastic process language with Hankel matrix of rank 3. This is an example where the minimal classic HMM (of order 3) is more complex than the equivalent QHMM. The quantum model \mathbf{Q} is defined as follows:

$$\mathbf{Q} = \{\Sigma, \mathcal{H}_S, \mathcal{T} = \{\mathcal{T} = \{T_a\}_{a \in \Sigma}, \}, \rho_0\},$$

where

- $\Sigma = \{0, 1, 2, 3\}$ is an alphabet of observable symbols.
- \mathcal{H}_S is a Hilbert space with dimension 2 (i.e. \mathbf{Q} is a 1 qubit quantum system).

- The operator-sum representation of \mathcal{T} is $\mathcal{T}_a = K_a \cdot K_a^\dagger$, where the Kraus operators are: $K_0 = \frac{1}{\sqrt{2}} |\uparrow\rangle\langle\uparrow|$, $K_1 = \frac{1}{\sqrt{2}} |\downarrow\rangle\langle\downarrow|$, $K_2 = \frac{1}{\sqrt{2}} |+\rangle\langle+|$, and $K_3 = \frac{1}{\sqrt{2}} |-\rangle\langle-|$.

- ρ_0 is the maximally entangled initial state.

We provide the following unitary definition of the same QHMM:

$$\mathbf{Q} = \{\Sigma, \mathcal{H}_S, \mathcal{H}_E, U, \mathcal{M}, \rho_0 \otimes |e_0\rangle\langle e_0|\},$$

where

- $\Sigma = \{0, 1, 2, 3\}$.
- \mathcal{H}_S is the state system Hilbert space with dimension 2.
- \mathcal{H}_E is the emission Hilbert space with dimension 4 (i.e. a 2 qubit quantum system with a measurement basis $\{e | e \in [0, 1, 2, 3]\}$), corresponding to the observable symbols.
- U is the unitary operation implemented by the “State transition” circuit in FIG 3.
- ρ_0 is the maximally mixed state implemented by the “Max mixed state” circuit in FIG 3.
- \mathcal{M} is the identity $\{0, 1, 2, 3\} \rightarrow \{0, 1, 2, 3\}$.

The circuit generating sequences with length 2 and their distribution are shown in FIG 3 and FIG 4. The “X” gates controlled on the classical “observable” registers o_0 and o_1 are used to reset the emission system to the initial state $|e_0\rangle$.

B. Primary and Measurement System Design. Test Case for the Ansatz Circuit Design

To get ideas for system design we refer to the theory of open quantum systems, which studies the system dynamics under the system-environment interaction [52]. Researchers consider Markovian and non-Markovian time evolutions [53, 54]. The precise definition of (non-) Markovianity is a subject of ongoing research [55, 56]. The major difference between these two evolution regimes are the memory effects in the non-Markovian case. Non-Markovian regime complicates the dynamics of the system, makes it irreversible, e.g. see [57]. The information in non-Markovian evolution flows from the system to the environment and from the environment to the system [58]. In real physical systems the description of the environment or even its dimension may not be known to us, however, in the present

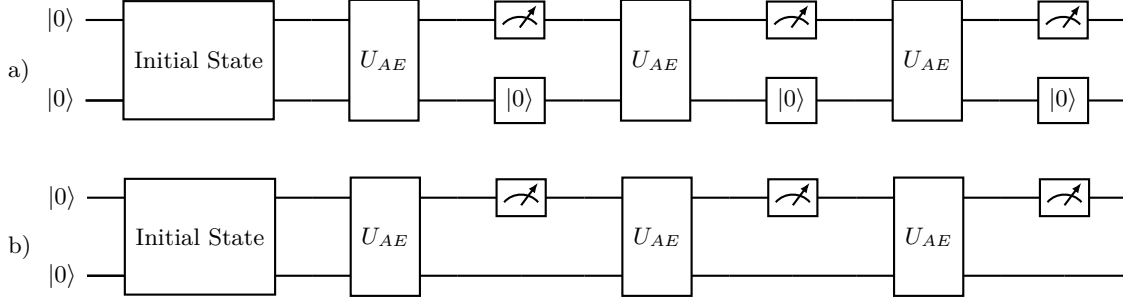


FIG. 5. QHMM Ansatz Circuit Design

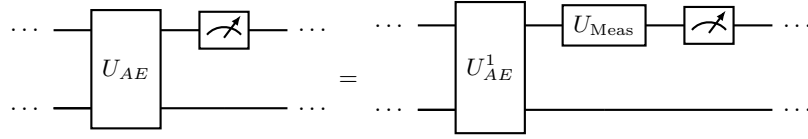


FIG. 6. Separated Measurement System Transformation

Based on the preliminaries in Section II B we can write the probability of a sequence for the circuit FIG 5 a) as

$$\Pr\{j_1 j_2 \dots j_k\} = \text{Tr} \left\{ M_{j_k} \sum_i K_i \dots M_{j_2} \sum_i K_i M_{j_1} \sum_i K_i \rho_A K_i^\dagger M_{j_1}^\dagger K_i^\dagger M_{j_2}^\dagger \dots K_i^\dagger M_{j_k}^\dagger \right\} \quad (64)$$

where M are projective measurements, and K are Kraus operators $K_i = (I \otimes \langle e_i |) U (I \otimes |e_0\rangle)$. Please, note that the same expression for the circuit FIG 5 b) would be much more complicated, since the start state e_0 of the environment may be changing between iterations creating a new set of Kraus operators each time.

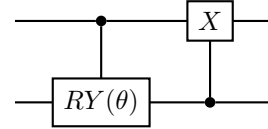
How do we know that the circuit on FIG 5 a) is able to produce probabilities according to the equation EQ 64? Here we suggest to use a well-known quantum operation - amplitude damping noise model [24, 59] as a test case and build a sequence generator. It is described by the following unitary transformation:

$$\mathbf{U}_{AD} = \begin{pmatrix} 1 & 0 & 0 & 0 \\ 0 & 0 & 0 & 1 \\ 0 & -\sqrt{\gamma} & \sqrt{1-\gamma} & 0 \\ 0 & \sqrt{1-\gamma} & \sqrt{\gamma} & 0 \end{pmatrix},$$

which, alternatively, can be represented in a circuit form:

$$\mathbf{U}_{AD} = (I \otimes |0\rangle\langle 0| + X \otimes |1\rangle\langle 1|) \times (|0\rangle\langle 0| \otimes I + |1\rangle\langle 1| \otimes RY(\theta))$$

or



where $\gamma = \sin^2(\frac{\theta}{2})$. The full circuit is shown on FIG 7.

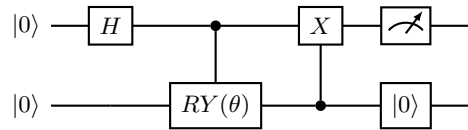


FIG. 7. Amplitude damping test case circuit for 1 step sequence

From this unitary we derive Kraus operators describing evolution of the principal subsystem given

that the start state of the environment is $e_0 = |0\rangle$:

$$\begin{aligned} \mathbf{K}_0 &= \\ &= \left(\begin{pmatrix} 1 \\ 0 \end{pmatrix} \otimes \begin{pmatrix} 1 & 0 \\ 0 & 1 \end{pmatrix} \right)^\dagger U \left(\begin{pmatrix} 1 \\ 0 \end{pmatrix} \otimes \begin{pmatrix} 1 & 0 \\ 0 & 1 \end{pmatrix} \right) \\ &= \begin{pmatrix} 1 & 0 \\ 0 & 0 \end{pmatrix}, \end{aligned}$$

$$\begin{aligned} \mathbf{K}_1 &= \\ &= \left(\begin{pmatrix} 0 \\ 1 \end{pmatrix} \otimes \begin{pmatrix} 1 & 0 \\ 0 & 1 \end{pmatrix} \right)^\dagger U \left(\begin{pmatrix} 1 \\ 0 \end{pmatrix} \otimes \begin{pmatrix} 1 & 0 \\ 0 & 1 \end{pmatrix} \right) \\ &= \begin{pmatrix} 0 & -\sqrt{\gamma} \\ 0 & \sqrt{1-\gamma} \end{pmatrix}. \end{aligned}$$

In this test case we want to compare the sequence probabilities calculated using EQ 64 with circuit (FIG 7) results, when it is run on the simulator and on *ibmq_montreal* hardware device. The probabilities calculated on the simulator will include shot, or sampling, noise. In order to reduce this error we use 100,000 shots. The hardware result will include both: hardware and shot noise. The circuit that was run on the simulator and *ibmq_montreal* hardware device is shown on FIG 8. Please note that the measurements are recorded on the classical register in reverse order following Qiskit's convention of putting the least significant bit to the right. Mid-circuit measurement and reset instructions have become available fairly recently in early 2021 [60]. They are now part of a broader dynamic circuit capability introduced in 2022 [61].

The comparison of the sequence probabilities is shown on FIG 9.

All calculations produce identical results up to sampling and hardware errors, so we confirm that our approach works as expected. It is worth noting that hardware results are very close to simulations. Here we have used *Sampler* primitive in *Qiskit Runtime* to run this experiment [62]. Behind the scenes this primitive implements error mitigation [63]. We have repeated the experiments for a range of γ parameters including the edges 0 and 1. In all cases, we observed the same level of agreement between the results.

The Hankel matrix for the current process is shown in Table II. The rank of the Hankel matrix changes with the length of the sequence (see FIG 10). It is interesting to note that if we choose a different start state on the quantum circuit - use excited state $|1\rangle$ instead of $|+\rangle$ state, then the Hankel matrix will have rank 2 for all sequences of length 2 and above.

IV. LEARNING QUANTUM HIDDEN MARKOV MODELS

In this section, we formalize and study the problem of learning QHMMs. The learning problem is defined as follows: given an empirical specification of a stochastic process language L , which is referred to as the learning target, the objective is to find a QHMM Q that is equivalent or approximates the sequence function f^L of the target. We discuss and formalize the components of the learning problem which include:

- Specification of the target stochastic language by estimating of its characteristics from the data. These characteristics may include order, Hankel matrix, finite distributions.
- Definition of a set of potential solutions or a hypotheses space of unitary QHMMs.
- Design of hypotheses' quality criteria or a fitness function.
- Design of learning algorithms.

A. Empirical Specification of Stochastic Languages

For every stochastic process language L we defined a sequence function f^L and corresponding generalized Hankel matrix H^L (8). Sequence function f^Q and Hankel matrix H^Q are defined for the language of every QHMM Q as well (31), (32). We assume that the target stochastic language is specified by a finite sample of the functional relation f^L , respectively a finite sub-matrix of H^L . If the sample is derived analytically or through exhaustive simulation of a known HMM, then its probabilities will be exactly the same as the probabilities of the target distribution. It is possible though, that the sample is derived through observation of a "natural" random source which is assumed to be Markovian. In this case the probabilities of the sample need to be estimated and this will have impact on the precision of the learned model. First, we discuss the size of a "representative" sample for a language or the *sample complexity* of the learning problem. It is known [44] that if a language L is defined by a classic HMM of order n then it is uniquely specified by the probabilities of all sequences up to length $2n - 1$. If the alphabet Σ contains m symbols this estimate defines a sample size of $\sum_{i=1}^{2n-1} m^i$ probabilities. If it is acceptable the specification to be valid for *almost all* HMMs-defined languages excluding a set with measure zero [45], then the representative sample would contain the probabilities of all sequences of length

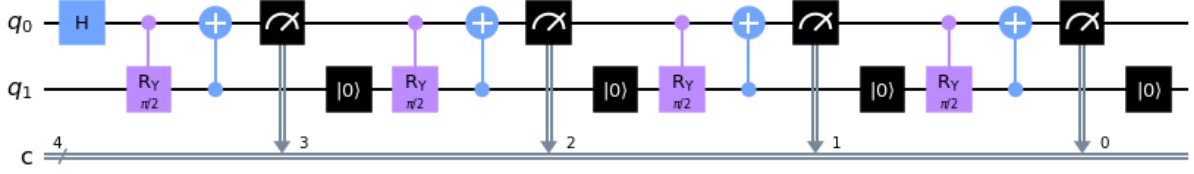
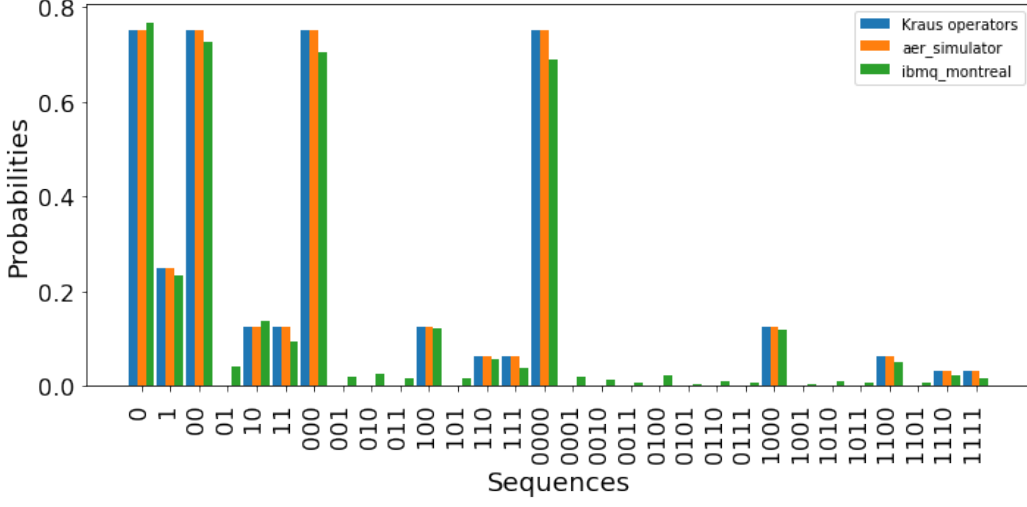
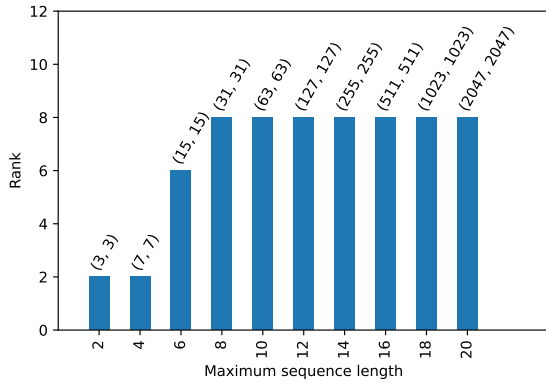
FIG. 8. Amplitude damping noise circuit in Qiskit. $\theta = \frac{\pi}{2}$ FIG. 9. Sequence probabilities for amplitude damping noise model. $\theta = \frac{\pi}{2}$ 

FIG. 10. Hankel matrix rank for different length sequences. Hankel matrix dimensions are shown in parentheses.

exactly $2l + 1$ where $l > 8 \lceil \log_m n \rceil$ or m^{2l+1} probabilities. In many learning scenarios, a classical HMM for the learning target is not provided, and in some cases, it is not known whether such an HMM exists. Instead, the only available training data consists of a

set of observed sequences, each of length T , sampled from an unknown process language L :

$$\mathcal{Y}^L = \{y_1, \dots, y_l : y_i \in \Sigma^T\}.$$

Using these empirical samples we have to estimate the sequence function (8) and then the order and the finite distributions of the unknown language. To estimate the sequence function for sequences with length k we construct the following set:

$$\mathbf{S}_k = \{\mathbf{a} : |\mathbf{a}| = k, \exists \mathbf{p}, \mathbf{s} \in \Sigma^*, \exists y \in \mathcal{Y}_L : \mathbf{p}\mathbf{a}\mathbf{s} = y\}. \quad (65)$$

If the sample \mathbf{S}_k contains m independently drawn sequences from the unknown distribution D_k^L , then the estimate $\hat{f}(\mathbf{a})$ is the empirical frequency of \mathbf{a} in \mathbf{S}_k :

$$\hat{f}(\mathbf{a}) = \frac{1}{m} \sum_{\mathbf{b} \in \mathbf{S}_k} \mathbf{1}_{\mathbf{a}}(\mathbf{b}).$$

The estimate of the finite distributions D_k^L is

$$\hat{D}_k^L = \{\hat{f}(\mathbf{a}) : \mathbf{a} \in \mathbf{S}_k\} \quad (66)$$

	empty	0	1	00	01	10	11
empty	1	0.75	0.25	0.75	0	0.125	0.125
0	0.75	0.75	0	0.75	0	0	0
1	0.25	0.125	0.125	0.125	0	0.0625	0.0625
00	0.75	0.75	0	0.75	0	0	0
01	0	0	0	0	0	0	0
10	0.125	0.125	0	0.125	0	0	0
11	0.125	0.0625	0.0625	0.0625	0	0.03125	0.03125

TABLE II. Hankel matrix of the amplitude damping process.

The approximation of the Hankel matrix is:

$$\hat{H}[\mathbf{u}, \mathbf{v}] = \hat{f}(\mathbf{u}\mathbf{v}), |\mathbf{u}\mathbf{v}| = k.$$

The error of this approximation depends on the sample size m [64] and is restricted as follows:

$$\|H - \hat{H}\| \leq \mathcal{O}\left(\frac{1}{\sqrt{m}}\right).$$

If we are given a sample \mathcal{Y}^L with no additional information we have to estimate a plausible order of the classical model by the maximum rank of the Hankel matrix. We start with low sequences length and estimate the rank increasing the length. If at particular sequence length the rank does not increase anymore we can use this rank as an estimate. This procedure will provide only local approximation since the problem to infer the rank of the Hankel matrix from data is undecidable [47].

B. QHMM Hypotheses Space

The hypotheses space \mathbb{Q} of the learning problem contains the unitary QHMMs (**Definition 3**):

$$\mathbb{Q} = \{\mathbf{Q} : \mathbf{Q} = (\Sigma, \mathcal{H}_S, \mathcal{H}_E, U, \mathcal{M}, \rho_0)\}, \quad (67)$$

where the parameters are specified and restricted by the given samples of the target stochastic process language:

- The alphabet Σ contains the observed m symbols.
- \mathcal{H}_S is a Hilbert space with dimension $\hat{N} = \lceil \sqrt{\hat{r}} \rceil$ where \hat{r} is the estimated maximal rank of the Hankel matrix built for the data sample \mathcal{Y} .
- \mathcal{H}_E is a Hilbert space with dimension $2^{\lceil \log_2 m \rceil} \leq M \leq \hat{N}^2$. We select any orthonormal basis $\mathcal{E} = \{|e_0\rangle \cdots |e_{M-1}\rangle\}$ of \mathcal{H}_E .

- U is a unitary operation on the Hilbert space $\mathcal{H}_S \otimes \mathcal{H}_E$ implemented by a quantum circuit of $\log_2 \hat{N} + \log_2 M$ qubits using gates from a base *gates type* set $\mathcal{G} = \{g_0 \cdots g_k\}$.
- \mathcal{M} is a bijective map $\mathcal{P}_m^E \rightarrow \Sigma$, where \mathcal{P}_m^E is an m -element partition of E .
- ρ_0 is initial state implemented as one of the following: the maximally entangled state, the maximally mixed state, or the ground state.

Every hypothesis \mathbf{Q} defines a sequence function $f^{\mathbf{Q}}$ and corresponding Hankel matrix $H^{\mathbf{Q}}$ which are used for evaluation of its quality. Every unitary operator U has representation as a quantum circuit \mathcal{C}_U with linear structure

$$\mathcal{C}_U = (g_i)_{i \geq 1}. \quad (68)$$

The quantum gates g_i are encoded as 3-tuples:

$$g = \langle \mathbf{t}, ([q_c,]q_d), ([p_1[, p_2]]) \rangle \quad (69)$$

where $\mathbf{t} \in \mathcal{G}$ is the gate's type, q_c and q_d are the control and data qubits, and p_1, p_2 are gate's parameters. We will make the assumption that the set of gate types \mathcal{G} includes single-qubit gates and two-qubit controlled gates.

Formally, the hypothesis space is the infinite set of all finite quantum circuits in the NM -dimensional Hilbert space $\mathcal{H}_S \otimes \mathcal{H}_E$, encoded as lists of gates (69).

C. Quality of a Hypothesis

1. Precision of a Hypothesis

A standard measure of the quality of a generative hypothesis Q defining language L^Q is its variational distance to the target distributions $D^L(1)$. Let's assume that the distributions D^L are defined by an unknown target QHMM model. The divergence between the target and the hypothesis for any sequence

$\mathbf{a} \in \Sigma^*$ can be defined as the divergence in probabilities assigned to the sequence \mathbf{a} by the target and the hypothesis(29):

$$\begin{aligned} \delta^{LQ}(\mathbf{a}) &= |P[\mathbf{a}|L] - P[\mathbf{a}|Q]| \\ &= |\text{tr}(T_{\mathbf{a}}^L \rho_0) - \text{tr}(T_{\mathbf{a}}^Q \rho_0)| \\ &= |\text{tr} \rho_{\mathbf{a}}^L - \text{tr} \rho_{\mathbf{a}}^Q|, \end{aligned} \quad (70)$$

where $\mathcal{T}^L = \{T_a^L\}_{a \in \Sigma}$ and $\mathcal{T}^Q = \{T_a^Q\}_{a \in \Sigma}$ are the quantum operations of the target model and the hypothesis and we assume a fixed initial state ρ_0 . The quantum states $\rho_{\mathbf{a}}^L = T_{\mathbf{a}}^L \rho_0$ and $\rho_{\mathbf{a}}^Q = T_{\mathbf{a}}^Q \rho_0$ represent the sequence generation paths under the target and the hypothesis models. The usual measurable distance between two quantum states is the *trace norm* $\|\rho_{\mathbf{a}}^L - \rho_{\mathbf{a}}^Q\|_1 = \text{tr} |\rho_{\mathbf{a}}^L - \rho_{\mathbf{a}}^Q|$. In the context of learning a QHMM, it is not feasible to directly measure the trace norm because the target model is generally unknown or may not even exist. The introduced divergence δ^{LQ} can be estimated empirically and is dominated by the theoretical trace norm:

$$\begin{aligned} \delta^{LQ}(\mathbf{a}) &= |\text{tr} \rho_{\mathbf{a}}^L - \text{tr} \rho_{\mathbf{a}}^Q| \\ &= \left| \sum_{i=1}^N (\rho_{\mathbf{a}}^L)_{ii} - (\rho_{\mathbf{a}}^Q)_{ii} \right| \\ &\leq \sum_{i=1}^N |(\rho_{\mathbf{a}}^L)_{ii} - (\rho_{\mathbf{a}}^Q)_{ii}| \\ &= \text{tr} |\rho_{\mathbf{a}}^L - \rho_{\mathbf{a}}^Q|. \end{aligned} \quad (71)$$

This relation will be used later in our analysis of QHMMs learning difficulty.

The divergence between the target language and the hypothesis on finite distributions of sequences with lengths exactly n is

$$\Delta_n(D^L || D^Q) = \max_{\mathbf{a} \in \Sigma^n} \delta^{LQ}(\mathbf{a}) \quad (72)$$

The average divergence between the hypothesis Q and the target L when given finite sample of sequences with lengths up to n is defined as

$$\Delta_{\leq n}(D^L || D^Q) = \frac{1}{n} \sum_{i=1}^n \Delta_i(D^L || D^Q) \quad (73)$$

We will refer to the average divergence (73) $\Delta_{\leq n}(D^L || D^Q)$ as the *empirical divergence* between a hypothesis and the learning target.

The *empirical divergence rate* of the hypothesis Q with respect to the target L is defined as

$$\hat{\Delta}(D^L || D^Q) = \lim_{n \rightarrow \infty} \Delta_{\leq n}(D^L || D^Q), \quad (74)$$

if the limit exists and it is finite.

We can prove that the empirical divergence rate between any QHMM hypothesis and a finite order stochastic process language converges with the increase of the sequences length n of the finite distributions in the learning sample.

Proposition 2. *If the learning target L is a finite order stochastic process language, then for any hypothesis $Q \in \mathcal{Q}$ the empirical divergence rate (74)*

$$\hat{\Delta}(D^L || D^Q) = \lim_{n \rightarrow \infty} \Delta_{\leq n}(D^L || D^Q)$$

exists and is finite.

Proof. For the finite order process languages the estimate of the relative entropy is consistent [65]:

$$\hat{D}_{KL}(D^L || D^Q) = \lim_{n \rightarrow \infty} \frac{1}{n} D_{KL}^n(D^L || D^Q) \quad (75)$$

where

$$D_{KL}^n(D^L || D^Q) = \sum_{\mathbf{a} \in \Sigma^n} P[\mathbf{a}|L] \log \frac{P[\mathbf{a}|L]}{P[\mathbf{a}|Q]}, \quad (76)$$

and the trace distance between the finite distributions is bounded by the relative entropy according to the Pinsker inequality:

$$D_{KL}(D^L || D^Q) \geq \frac{1}{2} D_{\text{tr}}^2(D^L || D^Q),$$

where

$$D_{\text{tr}}(D^L || D^Q) = \lim_{n \rightarrow \infty} D_{\text{tr}}(D_n^L || D_n^Q),$$

$$D_{\text{tr}}(D_n^L || D_n^Q) = \frac{1}{n} \sum_{i=1}^n d_{\text{tr}}(D_i^L || D_i^Q),$$

$$d_{\text{tr}}(D_i^L || D_i^Q) = \sum_{\mathbf{a} \in \Sigma^i} \text{tr} |\rho_{\mathbf{a}}^L - \rho_{\mathbf{a}}^Q|.$$

From the inequality in (71) follows

$$\begin{aligned} D_{KL}(D^L || D^Q) &\geq \frac{1}{2} D_{\text{tr}}^2(D^L || D^Q) \\ &\geq \frac{1}{2} \hat{\Delta}^2(D^L || D^Q), \end{aligned} \quad (77)$$

and we can conclude that the limit (74) exists in the cases when the target L is a finite order stochastic process language. \square

The empirical divergence rate (74) can be estimated from a sample of the target language and is considered to be the *precision* of a hypothesis

Q . This measure can be used in any approximate QHMM learning model even for languages which are not generated by any hypothesis in the space \mathbb{Q} .

Theoretically the divergence between the target L and a hypothesis Q defined by quantum operations \mathcal{T}^L and \mathcal{T}^Q (**Definition 2**) is the maximum probability divergence for sequences of length exactly $n, n > 0$ over all initial states ρ_0 is the trace norm defined as:

$$\|(\mathcal{T}^L)^n - (\mathcal{T}^Q)^n\|_1 = \max_{\rho} \|(\mathcal{T}^L)^n \rho - (\mathcal{T}^Q)^n \rho\|_1 \quad (78)$$

To estimate the relation between the trace divergence and the empirical divergence we consider the quantum states which define distributions over the sequences with length n :

$$\rho_n^i = (\mathcal{T}^i)^n \rho_0, \rho_0 \in D(\mathcal{H}_S), i = \{L, Q\}, \quad (79)$$

where ρ_0 is an initial state. The trace norm $\|\rho_n^L - \rho_n^Q\|_1$ is bounded from below by the empirical divergence (72) of Q as follows:

$$\begin{aligned} \|\rho_n^L - \rho_n^Q\|_1 &= \|(\mathcal{T}^L)^n \rho_0 - (\mathcal{T}^Q)^n \rho_0\|_1 \\ &= \max_{\mathbf{a} \in \Sigma^n} \|T_{\mathbf{a}}^L \rho_0 - T_{\mathbf{a}}^Q \rho_0\|_1 \\ &= \max_{\mathbf{a} \in \Sigma^n} \text{tr} |\rho_{\mathbf{a}}^L - \rho_{\mathbf{a}}^Q| \\ &\geq \max_{\mathbf{a} \in \Sigma^n} \delta^{LQ}(\mathbf{a}) \\ &= \Delta_n(D^L \| D^Q) \end{aligned} \quad (80)$$

From the inequality (80) follows that, given finite sample of sequences with length n , the empirical divergence between the hypothesis Q and the target L (72) is a lower bound of the trace divergence (78):

$$\Delta_n(D^L \| D^Q) \leq \|(\mathcal{T}^L)^n - (\mathcal{T}^Q)^n\|_1 \quad (81)$$

This inequality will be used to demonstrate a critical feature of the heuristic search approach to the learning of QHMMs: small changes in the norms of the unitary hypotheses lead to small changes of their precision.

2. Complexity of a Hypothesis

Another measure of quality is the hypothesis' complexity. If we assume that the state Hilbert space \mathcal{H}_S has fixed dimension N , where $N = \text{rank}(\hat{H}_L)$, then the free parameters of a hypothesis Q are the unitary U and the dimension of the emission component M . If for a unitary U we denote by $c_2(U)$ the number of two qubit gates then as a simple measure of its gate complexity we use the function:

$$C_g(Q) = \frac{c_2(U)}{\binom{NM}{2}}$$

The complexity of the unitary implementation is related also to the dimension of the emission system $\mathcal{H}_E, |\Sigma| \leq M \leq N^2$. The following measure reflects the dimension-related complexity:

$$C_e(Q) = \frac{M}{N^2}$$

The full complexity of a hypothesis is estimated as follows:

$$C(Q) = c_q C_g(Q) + c_e C_e(Q), \quad (82)$$

where c_q and c_e are real hyper parameters reflecting the trade-off between complex unitary or wider circuit.

We will integrate the hypothesis' precision (73) and complexity (82) measures into a single quality function called *fitness* which is defined as follows:

$$F(Q) = -(D^n(D_L \| D_Q) + C(Q)), \quad (83)$$

D. Formalization of the QHMM Learning Problem

We will discuss a specific formalization of the QHMM learning problem defined as follows:

Definition 4 (Unitary QHMM learning problem). *A Unitary Quantum HMM learning problem is defined as follows. Given:*

- A sample $\{D_t^L : 0 < t \leq n\}$ of the finite distributions of a unknown stochastic process language L (learning target),
- A unitary hypothesis space

$$\mathbb{Q} = \{Q : Q = (\Sigma, \mathcal{H}_S, \mathcal{H}_E, U, \mathcal{M}, \rho_0)\}$$

defined in Section IV B,

- A fitness function $F(Q)$ (83) defined over the hypothesis space,

find a hypothesis $Q^* \in \mathbb{Q}$ that maximizes the fitness function:

$$\mathbf{Q}^* = \underset{Q \in \mathbb{Q}}{\text{argmax}} F(Q). \quad (84)$$

The corresponding classical HMM learning problem is expected to be computationally hard [66], therefore we propose the optimization task (84) to be approached by heuristic search algorithms.

The heuristic search algorithms use the fitness function as a heuristic search function, providing information about the distance and direction towards the optimal solution. Therefore the properties of the fitness function are strongly related to the complexity of the learning task. To examine this relationship, we utilize the concept of a *fitness landscape*, which represents a multidimensional surface defined as follows:

$$\{F(Q) : Q \in \mathbb{Q}\}. \quad (85)$$

Intuitively, an optimization task is expected to be efficient, if the points on the fitness landscape are correlated with the optimal point or at least with the points in their neighbourhoods. This property requires the landscape to be *smooth* and any small change of a hypothesis Q results in restricted change of its fitness function. To formalize these intuitive notions, we introduce appropriate metrics in the hypothesis spaces \mathbb{Q} and in the fitness space.

The distance in the hypothesis space is quantified by the standard operator norm of the unitary operators. If Q_1 and Q_2 are two hypotheses with unitary operators correspondingly U_1 and U_2 (**Definition 4**), then the distance $\Delta Q^{12} = \Delta U^{12}$ is defined as follows:

$$\Delta Q^{12} = \|U_1 - U_2\|. \quad (86)$$

According to the *genetic algorithms'* terminology, the distance in the hypothesis representation space is called *genotypes* distance.

To introduce distance in the fitness space, we note that the unitary HQMMs representations are defined in a larger Hilbert space (by tensoring an emission system) and use a *stabilized* version of the trace norm known as *diamond norm* [67]:

$$\|\mathcal{T}\|_{\diamond} = \max_{\rho \in D(\mathcal{H}_S \otimes \mathcal{H}_S)} \|(\mathcal{T} \otimes I_N)\rho\|_1. \quad (87)$$

In the diamond norm definition the dimension of the emission system M is equal to the dimension of the state system N , since the increase of $M > N$ cannot increase the trace norm. The diamond norm induces distance between the probabilities of 1-symbol sequences generated by the hypotheses Q_1 and Q_2 :

$$\begin{aligned} \Delta \mathcal{T}^{12} &= \|\mathcal{T}^1 - \mathcal{T}^2\|_{\diamond} \\ &= \max_{\rho \in D(\mathcal{H}_S \otimes \mathcal{H}_S)} \|(\mathcal{T}^1 - \mathcal{T}^2) \otimes I_N \rho\|_1, \end{aligned}$$

which we call a *phenotypes* distance. Since the diamond norm is a stabilized version of the trace norm (Lemma 12, [67]) we have the inequality:

$$\|(\mathcal{T}^1 - \mathcal{T}^2)\|_1 \leq \|\mathcal{T}^1 - \mathcal{T}^2\|_{\diamond}, \quad (88)$$

and from inequality (81) follows, that the average divergence between the hypothesis Q_1 and Q_2 on finite sample of sequences with length 1 is a lower bound of the diamond norm:

$$\Delta_1(D^1 \| D^2) \leq \|\mathcal{T}^1 - \mathcal{T}^2\|_{\diamond}. \quad (89)$$

The introduced distances in hypothesis and fitness spaces imply smooth fitness landscape for the single-symbol sequences, due to the Continuity of Stinespring's representation Theorem [40]. According to the Theorem, two quantum operations $\mathcal{T}^1, \mathcal{T}^2$, respectively two QHMMs, are close in diamond norm iff they have unitary representations which are close in operator norm:

$$\frac{1}{2} \Delta \mathcal{T}^{12} \leq \Delta U^{12} \leq \sqrt{\Delta \mathcal{T}^{12}} \quad (90)$$

This inequality suggests that the operator norm difference between the hypotheses dominates the trace (88) and average (89) empirical divergences of their single-symbol distributions:

$$\frac{1}{2} \Delta_1(D^1 \| D^2) \leq \frac{1}{2} \|\mathcal{T}^1 - \mathcal{T}^2\|_1 \leq \Delta U^{12}. \quad (91)$$

The distributions over sequences with any finite length n are generated by the n -th powers of the quantum operations (29) and their unitary dilations:

$$(\mathcal{T}^i)^n \rho_0 = U_i^n \rho_0 U_i^{\dagger n}, \rho_0 \in D(\mathcal{H}_S), i \in 1, 2. \quad (92)$$

The operator-norm distance between the unitary operators defining n -symbol sequences is related to the genotypes' distance $\Delta Q^{12} = \|U_1 - U_2\|$ as follows:

$$\begin{aligned} \|U_1^n - U_2^n\| &= \left\| (U_1 - U_2) \sum_{k=1}^n U_1^{n-k} U_2^{k-1} \right\| \\ &\leq \|U_1 - U_2\| \left\| \sum_{k=1}^n U_1^{n-k} U_2^{k-1} \right\| \\ &\leq \|U_1 - U_2\| \left(\sum_{k=1}^n \|U_1^{n-k} U_2^{k-1}\| \right) \\ &\leq n \|U_1 - U_2\|. \end{aligned} \quad (93)$$

For the case of quantum operations defining n -symbol sequences, and accounting that the diamond norm is stabilized trace norm, from the Continuity Theorem (91) follows:

$$\frac{1}{2} \|(\mathcal{T}^1)^n - (\mathcal{T}^2)^n\|_1 \leq \|U_1^n - U_2^n\|. \quad (94)$$

By applying (93) and (71),(72) to (94) we can derive an upper bound estimate for the n -symbol distributions divergence in terms of genotypes' distance in the hypothesis space:

$$\frac{1}{2n} \Delta_n(D^1 \| D^2) \leq \frac{1}{2n} \|\mathcal{T}_1^n - \mathcal{T}_2^n\|_1 \leq \Delta U^{12} \quad (95)$$

The empirical divergence of a learning sample of sequences with lengths up to n is bounded as follows:

$$\frac{1}{2n} \sum_{i=1}^n \frac{1}{i} \Delta_i(D^1||D^2) \leq \Delta U^{12} \quad (96)$$

This inequality allows the precision component in the fitness distance between of two hypotheses to be estimated by the operator norm distance of their unitary representations(73) :

$$\Delta_{\leq n}(D^1||D^2) = \frac{1}{n} \sum_{i=1}^n \Delta_i(D^1||D^2) \quad (97)$$

By replacing the harmonic weight $\frac{1}{i}$ of the divergence in (96) by $\frac{1}{n}$ and applying (97):

$$\Delta_{\leq n}(D^1||D^2) \leq \sum_{i=1}^n \frac{1}{i} \Delta_i(D^1||D^2)$$

we derive the estimate:

$$\frac{1}{2n} \Delta_{\leq n}(D^1||D^2) \leq \Delta U^{12} \quad (98)$$

Inequality (98) demonstrates that the fitness landscape of the QHMMs learning problem is smooth: for every two unitary hypothesis close in genotype distance (operator norms) the corresponding phenotypes' distance (empirical distributions divergence) for any sequences length n is restricted.

To experimentally investigate the difficulty of the heuristic approach to the QHMM learning task we estimate the landscape properties of the the QHMM learning problem discussed in Example 3. The dependency between the change in the operator norm and the corresponding divergence of the sequence distributions is estimated by a random walk starting at the optimal hypothesis Q^* with unitary $U^* = U_0$. A new unitary is generated at every step $t = 1, 2, \dots$ by random single parameter mutation with standard deviation 10%. The expected fitness divergences (phenotypes distance) $\Delta_n(D^*||D^t)$ (72) for sequences with lengths $n \in [2..5]$, and the expected total fitness divergence $\Delta_{\leq 5}(D^*||D^t)$ (97) conditioned on the genotypes distance (86) $\Delta U = \|U^* - U_t\|, \Delta U \in [0, 1]$ are shown on FIG 11.

On FIG 12 we present estimations of the Pearson correlation coefficient of the fitness of a hypothesis and its distance to the optimal solution for sequences with length up to 5 symbols:

$$r = \frac{\text{cov}(\Delta_{\leq 5}(D^*||D^t), \Delta U)}{\text{std}(\Delta_{\leq 5}(D^*||D^t))\text{std}(\Delta U)} \quad (99)$$

The coefficient is estimated for three mutation rates and can be used as measure of the expected effectiveness of the evolutionary algorithms applied to the QHMM learning problem.

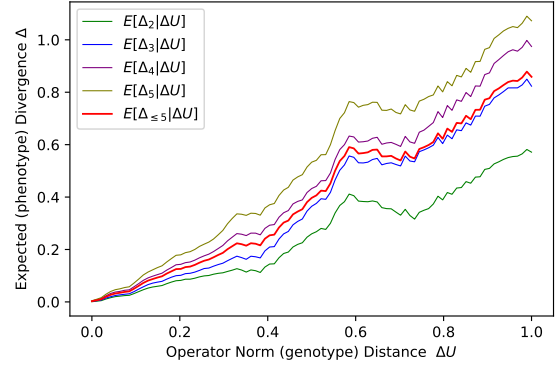


FIG. 11. Smoothness of Fitness Landscape

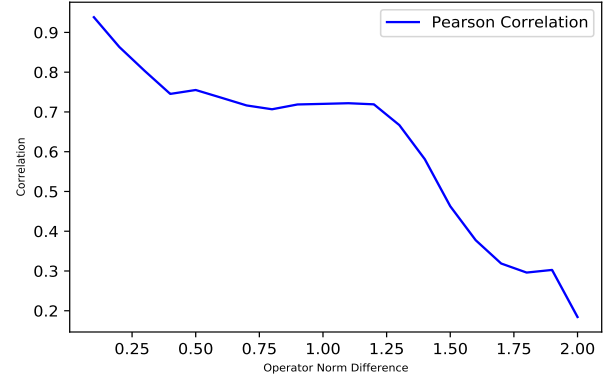


FIG. 12. Correlation of Fitness Landscape

E. QHMM Learning Algorithm

The learning algorithm takes as input an estimation of the Hankel matrix associated with the unknown process language $\hat{H}^L \in R^{\Sigma^{\leq n} \times \Sigma^{\leq n}}$ and the specification of a hypothesis space \mathbb{Q} . Two of the components of the hypothesis space are fixed by the Hankel matrix \hat{H}^L : the alphabet Σ and the dimension of the state Hilbert space \mathcal{H}_S which is $\hat{N} = \text{rank}(\hat{H}^L)$. The free parameters, subject of optimization, are the dimension M of the emission Hilbert space \mathcal{H}_E , the unitary U , the mapping \mathcal{M} , and the type of the initial density ρ_0 . In order to simplify the discussion and focus on the essential part of the algorithm, we will assume that only the unitary transformation U will be learned.

The hypothesis space \mathbb{Q} comprises both discrete and continuous components, represented by structural and parametric subspaces. The structural subspace contains the non-parametric parts $g = \langle\langle t \rangle\rangle, \langle\langle q \rangle\rangle, \langle\langle \cdot \rangle\rangle$ of the linear quantum circuits' $\{\mathcal{C}_U\}$ as

defined in (68). The parametric subspace is defined by vectors $\{\mathcal{P}_U\}$ with circuit gates' parameters:

$$\mathcal{P}_U = \{p : \exists g \in \mathcal{C}_U, g = \langle (\cdot), (\cdot), (p) \rangle\}.$$

The algorithm performs evolutionary global search in the structural subspace as the fitness of every circuit structure is estimated by parametric optimization of (83):

$$Fit(\mathcal{C}_U) = \max_{\mathcal{P}_U} F(Q_U), \quad (100)$$

where \mathcal{C}_U is the unitary encoding of the hypothesis Q_U . The optimal parameters $P_U^* = \underset{\mathcal{P}_U}{\operatorname{argmax}} F(Q_U)$ of every hypothesis Q_U are calculated by local multivariate nonlinear optimization procedure. Derivative-free solvers as *Powell, TNC, Cobyla* as well as gradient-based *BFGS, GC, SLSQP* have been used. The type of solver for each structure optimization is selected by an adaptive local search optimization procedure. After the optimization the optimal parameters P_U^* become parameters of the hypothesis and the optimal fitness value becomes fitness of the hypothesis. The combination of evolutionary global search in the space of quantum circuit structures and local parametric optimization classifies our learning method as *Lamarckian learning* [68].

Algorithm 2: Random Hypothesis

```

procedure RANDOMGATE(Q)
   $t \sim \text{gatesDistribution}(\mathcal{G})$ 
  /* Select gate's type */
   $q_c, q_d \sim \text{qubitsDistribution}(N, M)$ 
  /* Select control and data qubits */
   $p_1, p_2 \sim \text{parametersDistribution}([0, 8\pi])$ 
  /* Select gate parameters */
   $gate \leftarrow \langle t, (q_c, q_d), (p_1, p_2) \rangle$ 
  /* Create a gate */
  return gate

procedure RANDOMHYPOTHESIS(Q)
   $minGts, maxGts \leftarrow const_1, const_2$ 
  /* Min-Max number of gates */
   $numGts \sim \text{Uniform}(minGts, maxGts)$ 
  /* Random number of gates */
   $C \leftarrow []$ 
  /* Initial circuit for the hypothesis */
  for  $g = 1$  to  $numGts$  do
     $C \leftarrow C + [\text{RANDOMGATE}(Q)]$ 
   $\mathcal{P}_C^* \leftarrow \underset{\mathcal{P}_C}{\operatorname{argmax}} F(C)$  /* Find parameters
   $\mathcal{P}_C^*$  of  $C$  which maximize the fitness */
   $F_C \leftarrow F(\mathcal{P}_C^*)$  /* Fitness value of  $C^*$  */
  return  $C^*$ 

```

Algorithm 3: Evolutionary Learning

```

Input :  $\mu, \lambda, \mathbb{Q}$  (67),  $F(Q)$  (83),  $F^*$ ,  $gMax$ ,  $\mathcal{G}$ 
Output: Best Hypothesis  $Q^* = \underset{Q \in \mathbb{Q}}{\operatorname{argmax}} F(Q)$ 

Initialize
  •  $g \leftarrow 0$  /* Evolutionary generation */
  •  $t \leftarrow 0$  /* Search progress steps */
  •  $P_g \leftarrow \text{RANDOM}(\mu, \mathbb{Q})$  /* Initial
  population:  $\mu$  random hypotheses */

while  $\max_{Q \in P_g} F(Q) < F^*$  and  $g < gMax$  do
   $\tau \leftarrow \text{Temperature}(t)$ 
   $Parents \leftarrow$ 
  Select( $P_g, \lambda, selectionDistribution$ )
   $Children \leftarrow$ 
  Modify( $Parents, \tau, modificationDistributions$ )
   $P_{g+1} \leftarrow \text{Select}(P_g \cup$ 
   $Children, \mu, survivalDistribution)$ 
   $g \leftarrow g + 1$ 
  /* Check for search progress during
  last progWin steps */
  if noProgress(progWin) then
    |  $t \leftarrow 0$ 
  else
    |  $t \leftarrow t + 1$ 
   $Distributions \leftarrow \text{Adapt}(Distributions)$ 

return  $\underset{Q \in P_g}{\operatorname{argmax}} F(Q)$ 

```

Algorithm 4: Mutate a Hypothesis

```

procedure MUTATEHYPOTHESIS( $C, pos,$ 
 $mType$ )
  switch  $mType$  do
    when "gte" :
       $C[pos].gate \sim \text{gatesDistribution}(\mathcal{G})$ 
      /* Mutate gate's type */
      when "qbt" :  $C[pos].qubits \sim$ 
       $\text{qubitsDistribution}(N, M)$  /* Mutate
      gate's qubits */
      when "rpl" :
       $C[pos] \leftarrow \text{RANDOMGATE}(Q)$  /* Replace
      gate */
      when "dlt" :  $C[pos:] \leftarrow C[pos + 1:]$ 
      /* Delete gate */
      when "ins" :  $C \leftarrow C[:$ 
       $pos] + [\text{RANDOMGATE}(Q)] + C[pos:]$ 
      /* Insert gate */
  return  $C$ 

```

The algorithm starts with random generation of a finite sample of μ hypotheses forming the initial *population* (Algorithm 2). The process of iterative improvement of the population consists of three base randomized steps, including selection of set of existing hypotheses to be improved referred to as parents, modification of the parents to generate offspring or children, selection from the parents and children a new generation of the popula-

Algorithm 5: Hypothesis Modification

```

procedure MODIFYHYPOTHESIS( $\mathcal{C}$ )
   $C_{best} \leftarrow \mathcal{C}$  /* Current best hypothesis */
   $C_{current} \leftarrow \mathcal{C}$  /* Current hypothesis */
   $searchSteps \sim \text{localSearchLen}(1..max)$ 
  /* Random local search steps */
  for  $step = 1$  to  $searchSteps$  do
     $sType \sim \text{localSearchType}(\text{"depth"}, \text{"breadth"})$ 
    /* local search type */
     $mProb \sim \text{mutationRate}(0.1, \dots, 0.5)$ 
    /* Mutation rate */
     $\mathcal{C} \leftarrow C_{current}$  /* Current hypothesis to search around */
    for  $pos = 1$  to  $\text{Size}(\mathcal{C})$  do
      if  $\text{RANDOM} > mProb$  then
         $mType \sim \text{mutationType}(\text{"gte"}, \dots, \text{"ins"})$ 
        /* Mutation type */
         $\text{MUTATEHYPOTHESIS}(\mathcal{C}, pos, mType)$ 
        /* Mutate hypothesis at pos */
       $\mathcal{P}_{\mathcal{C}}^* \leftarrow \text{argmax}_{\mathcal{P}_{\mathcal{C}}} F(\mathcal{C})$  /* Find parameters  $\mathcal{P}_{\mathcal{C}}^*$  which maximize the fitness */
       $F_{\mathcal{C}} \leftarrow F(\mathcal{C})$  /* Fitness value of  $\mathcal{C}$  with optimal parameters  $\mathcal{P}_{\mathcal{C}}^*$  */
      if  $F(\mathcal{C}) > F(C_{best})$  then
         $C_{best} \leftarrow \mathcal{C}$  /* Save the new best hypothesis */
      if  $\text{ACCEPT}(F(\mathcal{C}), F(C_{current}), \text{Temperature})$  then
         $C_{current} \leftarrow \mathcal{C}$  /* New current hypothesis */
    if  $\text{ACCEPT}(F(\mathcal{C}), F(C_{best}), \text{Temperature})$  then
       $C_{best} \leftarrow \mathcal{C}$  /* new preferred hypothesis */
  return  $C_{best}$ 

```

tion (Algorithm 3). The modification operations include range of hypothesis mutations (Algorithm 4) utilized by a stochastic local search (Algorithm 5). Since the random operations selecting offspring and survivors are biased towards hypotheses with higher fitness (*survival of the fittest*), the entire population evolves towards regions of the space \mathbb{Q} which contain better potential solutions and eventually

an optimal solution. The trade-off between exploration and exploitation within a hypothesis space region is controlled by a global variable referred to as *Temperature*. The temperature defines the probability of accepting a new hypothesis, even if it is not superior to its parent. The temperature gradually decreases with the search progression, thereby increasing the likelihood of selecting only better solutions. If a certain threshold of steps is reached without any fitness improvement, the temperature is reset to its highest value to allow exploration of new regions. The temperature(τ) is calculated as a function of the number of steps t (FIG (13)) as follows:

$$\tau = (t^{\frac{3}{2}} + 1)^{-\frac{1}{4}}.$$

The probability a new hypothesis with fitness F_{new} to be accepted instead of its superior parent with fitness $F_{old} \geq F_{new}$ at temperature τ is defined by:

$$P_{new} = \exp\left(\frac{0.6 F_{old} - F_{new}}{\tau F_{old}}\right)$$

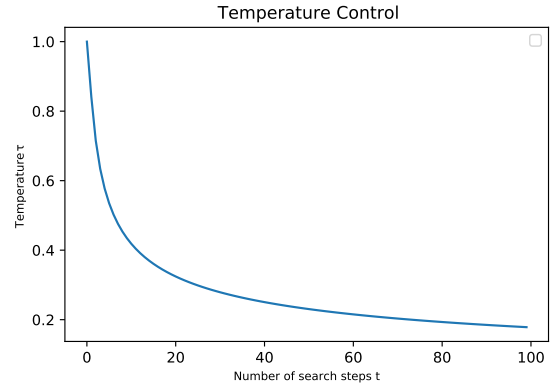


FIG. 13. Temperature control

The control of hypothesis acceptance probability by the global temperature τ is illustrated FIG 14.

The selection of a set of hypotheses, referred to as parents, to be modified and evaluated as potential new members of the population relies on the fitness of these hypotheses. The candidates with better fitness are more likely to be selected for further consideration. This approach can be successful in case of unimodal landscapes. However, if the fitness landscape is rugged, characterized by numerous local extrema, employing a uniform, strong selection pressure strategy can result in premature convergence towards a local solution. Therefore, in our algorithm

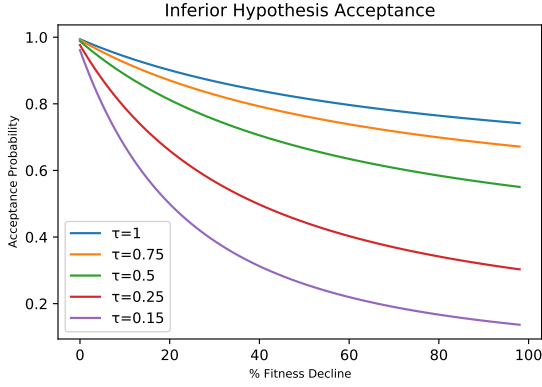


FIG. 14. Inferior Hypotheses Acceptance

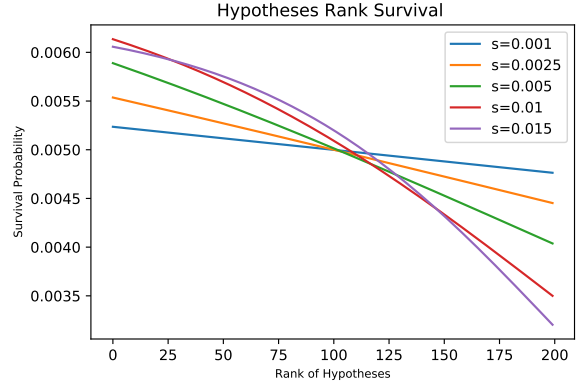


FIG. 16. Rank Survival Distributions

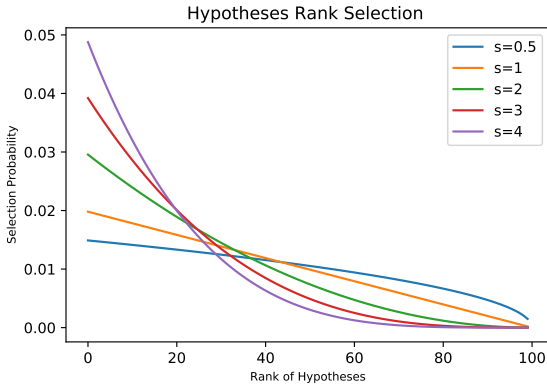


FIG. 15. Rank Selection Distributions

we use selection distributions based on rank, fitness, and tournaments. Every selection distribution type is used with up to 5 levels of selection pressure. For example, let's consider rank-based selection where the hypothesis are ranked according their fitness values with the fittest hypothesis receiving the lowest rank. Then the probability a hypothesis with rank i to be selected for offspring generation is:

$$P_{selection}[Q_i] = \frac{(\mu - i)^s}{\sum_{r=1}^{\mu} (\mu - r)^s},$$

where μ is the size of the population and s is a parameter called *selection strength*. The shape of the rank selection distribution for different values of the parameter is shown on FIG 15.

The survival distributions define the chance a hypothesis - old or newly generated - to participate in the new generation. These distributions are also based on rank and fitness and use up to 5 levels of selection pressure. The probability a hypothesis with rank i to be selected to "survive" in the next

generation is:

$$P_{survival}[Q_i] = \frac{(d_i + 1)^{-1}}{\sum_{r=1}^{\mu} (d_r + 1)^{-1}}, \quad (101)$$

where

$$d_r = \exp\{s(r - \mu - \lambda)\}, \quad (102)$$

μ is the size of the population, λ is the size of the offspring, and s is a parameter called *survival strength*. The shape of the rank survival distribution for different values of the parameter is shown on FIG 16.

The evolutionary algorithm uses multiple distributions to implement the processes of selection, modification, and survival (TABLE III). The parameters of these distributions along with the population size μ and the offspring size λ are referred to as *hyperparameters* of the algorithm. The hyperparameters are critical for the performance of the algorithm. Since each learning task is unique and the fitness landscape can change during the evolutionary process, it is essential to dynamically adjust the hyperparameters as the learning evolves. To achieve adaptive control over the hyperparameters, we employ a reinforcement learning algorithm based on the "multi-armed bandit model". This algorithm effectively addresses the exploration-exploitation trade-off, and maximizes the cumulative reward obtained through the parameters adaptation. Let's assume that the evolutionary algorithm utilizes a procedure or distribution $A(h)$ which depends on a parameter $h \in \{h_1, \dots, h_k\}$. For a generation t we define a distribution $D_t^h = \{p_i : p_i = P[h_i]\}$. Every time when A is used during the generation t we first sample a value $h \sim D_t^h$ and then use it for this particular activation $A(h)$. We register if the particular usage of $A(h)$ has been successful or not. Success is considered when the fitness of a hypothesis or a population has increased and in this case the value

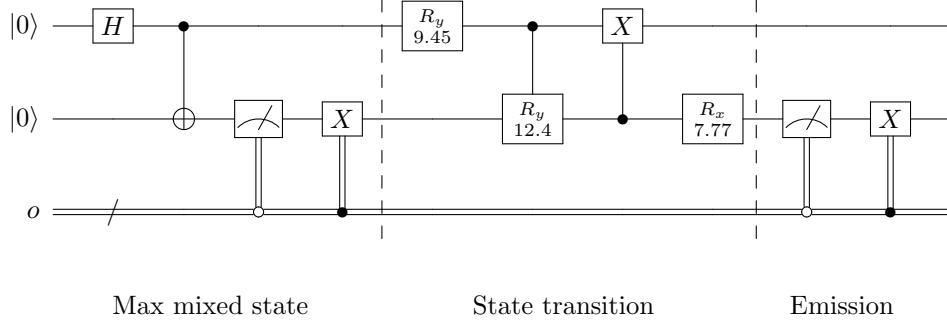


FIG. 17. QHMM Defining Market Distribution

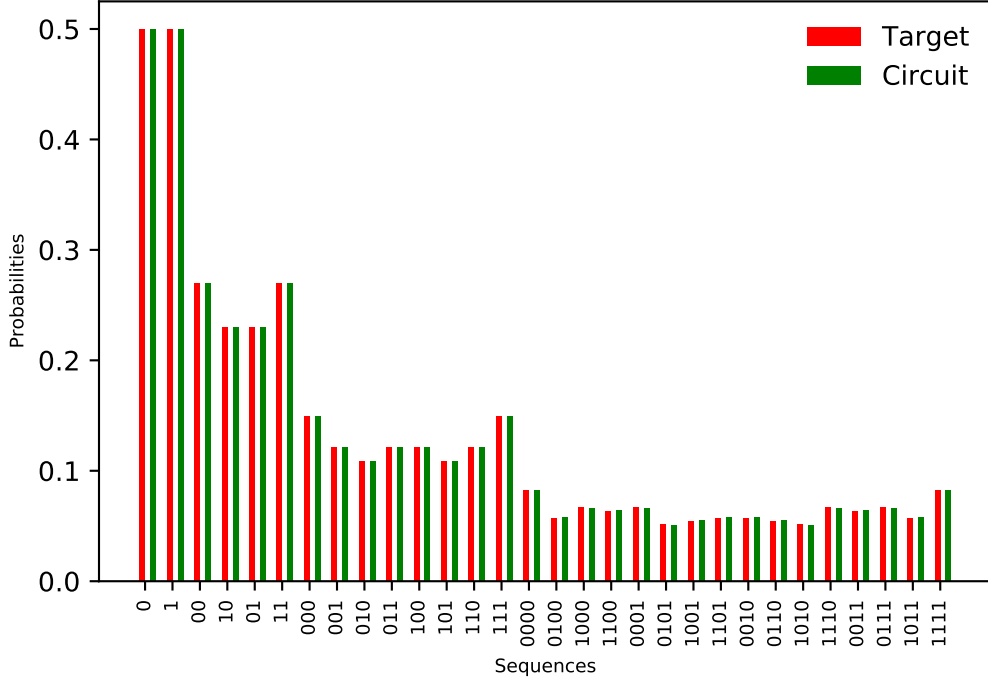


FIG. 18. Targeted and Learned Market Distributions

of h receives reward 1. in the end of the generation t we will have a reward vector $\mathbf{r}_t = [r_t^1, \dots, r_t^k]$, where r_t^j is the number of times the usage of the value $h = h_j$ during the generation t has resulted in fitness improvement. Let the initial distribution be the uniform distribution $D_0^h = \{\frac{1}{k}, \dots, \frac{1}{k}\}$. The

distribution at generation $t+1$ is defined as follows:

$$D_{t+1}^h = \left\{ p_i : p_i = \gamma \frac{1}{k} + (1-\gamma) \frac{r_t^i}{\sum_{j=1}^k r_t^j}, i = [1, k] \right\},$$

where $\gamma \in [0, 1]$ quantifies the trade-off between exploration and exploitation. The pseudo code of the algorithm is presented as Algorithm 3.

<i>Distribution</i>	Description	Domain
selectionDistributionTypes	Probabilities of selection types.	[<i>Fitness, Rank, Tournament</i>]
selectionDistributionStrength	Probabilities of selective pressure levels	[0.1, 0.2, 0.5, 0.7, 1]
survivalDistributionTypes	Probabilities of survival types	[<i>Fitness, Rank</i>]
survivalDistributionStrength	Probabilities of survival pressure levels.	[0.1, 0.2, 0.5, 0.7, 1]
gatesDistribution	Probabilities of gate types	$\mathcal{G} = \{g_0 \cdots g_k\}$
qubitsDistribution	Probabilities of qubits	$[1, n + m], P(n + m, 2)$
localSearchLen Distribution	Probabilities of local search steps	[1, 10]
localSearchType Distribution	Probabilities of local search types	[<i>depth, breadth</i>]
mutationRate Distribution	Probabilities of hypothesis' mutation rates	[0.1, ...0.5]
mutationType Distribution	Probabilities of hypothesis' mutation types	[<i>'gte', 'qbt', 'rpl', 'dlt', 'ins'</i>]
optimizationAlgs Distribution	Probabilities of nonlinear solvers	[<i>'tnc', 'cbla', 'bfsq', 'gc', 'slsqp'</i>]

TABLE III. Adaptive distributions used by the evolutionary algorithm

Example 3. In this example we apply the QHMM learning algorithm to the Market classical HMM discussed in **Example 1**. The minimal order of the classical model estimated using the Hankel matrix is: $n = 4$. The learning sample as distributions of sequences with lengths up to $t = 2n - 1 = 7$ was generated using the string function of the classic model (EQ 5). The QHMM sequences distribution is generated using the sequence function (EQ 5). The preliminary model specification based on the learning sample analysis is the following:

$$\mathbf{Q} = \{\Sigma, \mathcal{H}_S, \mathcal{H}_E, U, \mathcal{M}, \rho_0\}$$

where $\Sigma = \{0, 1\}$, \mathcal{H}_S is a Hilbert space with dimension $N = \sqrt{n} = 2$ (i.e. 1 qubit quantum system), \mathcal{H}_E is a Hilbert space with dimension 2 (i.e. 1 qubit quantum system and the measurement basis is $\{[0], [1]\}$), U is a unitary operation on the Hilbert space $\mathcal{H}_E \otimes \mathcal{H}_S$ implemented by quantum gates in $\mathcal{G} = \{X, Y, RX, RY\}$, and ρ_0 is the tensor product of uniformly distributed state and grounded emission systems.

Exact match (i.e zero-divergence between classic and quantum distributions) was reached in average of 150 iterations by population of 100 solutions. The best solution is shown in FIG 17. Part of the target and learned distributions at the end of the search are shown in FIG 18.

In the next example we demonstrate that the QHMMs are efficient generators of stochastic mixtures of distributions.

Example 4. Let's consider a process each point of which is drawn from a Normal distribution belonging to a finite set of Normal distributions:

$$\{Y_t : Y_t \sim \mathcal{N}(\mu, \sigma^2(s), s \in S)\},$$

where $S = \{s_1, \dots, s_N\}$ is a finite set of unobservable states. The classical HMM of such a process with $n=4$ hidden states, defining standard deviations correspondingly [0.5, 1, 2, 4] is specified in Table IV. The model is minimal and in each state $s \in S$ an integer observable in the interval $[0, 3]$ is emitted by sampling from a normal distribution $\mathcal{N}(\mu = 1.5, \sigma(s))$ as shown in FIG 19. The learning sample is a set of distributions of sequences with lengths up to $t = 2N - 1 = 7$. It was generated using the string function of the classic model (EQ 5). The preliminary model specification based on the learning sample analysis is the following:

$$\mathbf{Q} = \{\Sigma, \mathcal{H}_S, \mathcal{H}_E, U, \mathcal{M}, \rho_0\}$$

where $\Sigma = \{0, 1\}$, \mathcal{H}_S is a Hilbert space with dimension $N = \sqrt{n} = 2$ (i.e. 1 qubit quantum system), \mathcal{H}_E is a Hilbert space with dimension 4 (i.e. 2-qubit quantum system and the measurement basis is $\{[0, 0], [0, 1], [1, 0], [1, 1]\}$), U is a unitary operation on the Hilbert space $\mathcal{H}_E \otimes \mathcal{H}_S$ implemented by quantum gates in $\mathcal{G} = \{X, Y, RX, RY, P\}$, and ρ_0 is the tensor product of maximally mixed state system and grounded emission systems. Divergence error less than 0.01% was reached in average of 250 iterations by population of 150 hypotheses. The best solution is shown in FIG 20. Part of the target and learned distributions at the end of the search are shown in FIG 21.

F. Learning QHMM with Ansatz Circuits

In this paper, we propose the following algorithm for learning *quantum hidden Markov model* using ansatz circuits.

S	Description	S	0	1	2	3	S	0	1	2	3
0	Low Variance	0	0.60	0.25	0.05	0.10	0	0.00	0.50	0.50	0.00
1	Low-Medium Variance	1	0.05	0.15	0.05	0.75	1	0.01	0.49	0.49	0.01
2	Medium-High Variance	2	0.75	0.05	0.15	0.05	2	0.13	0.37	0.37	0.13
3	High Variance	3	0.10	0.05	0.65	0.20	3	0.22	0.28	0.28	0.22

TABLE IV. Gaussian Mixture HMM. Left: Hidden States Descriptions. Center: States Transition Probabilities. Right: Emission Probabilities.

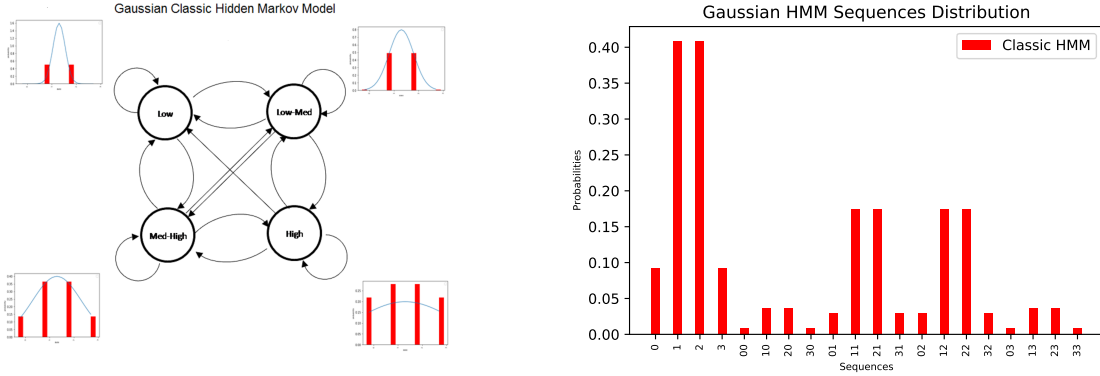


FIG. 19. Gaussian Mixture HMM

Algorithm 6: Quantum Hidden Markov Model Learning with Ansatz Circuits

- Input :** table of observed sequences and corresponding probabilities, min-max sequence length (optional)
- Output:** trained circuit that can be extended to the required sequence length
- 1 Initialize start state, variational quantum ansatz circuit, start values of the parameters. Multiple options for start states and ansatz circuits are discussed in Section III B.
 - 2 $Cost = \sum_i l_i \times (p_i^{target} - p_i^{current})^2$ where l_i is the sequence length
 - 3 Find optimal parameters for quantum circuit with classical technique, e.g. Nelder-Mead method.
-

This approach essentially utilizes the training of parameterized quantum circuits to model sequence data.

G. Ansatz Circuit Template

The topic of efficient ansatz selection is an area of active research [69–73].

Due to the presence of noise in quantum devices, one must select an ansatz which is sufficiently ex-

pressive (i.e. able to access the solution space in the Hilbert space) while maintaining a low parameter count and lower depth of the quantum circuits in order to suppress the noise.

Moreover, the proposed ansatz should contain sufficient entanglement to be non-simulable on a classical computer. Qiskit provides a variety of built-in ansatz templates with various combinations of the number of parametric gates and the circuit depth [74]. The two ansatz circuits we test in this work are *RealAmplitudes* (FIG 22) and *EfficientSU2* (FIG 23 and FIG 24). We consider two variations for *EfficientSU2* ansatz circuit: 1) with R_y, R_z (FIG 23) and 2) with R_z, R_x (FIG 24) rotation gates. Furthermore, in the entanglement block we test full and linear entanglement schemes. The latter scheme is more hardware efficient as it doesn't assume fully connected mapping between qubits.

V. EXAMPLES OF QHMMS

A. Simple Four Symbol Stochastic Process

Let's consider a process defined by the following Kraus operators [25]:

$$\frac{1}{\sqrt{2}}|0\rangle\langle 0|, \frac{1}{\sqrt{2}}|1\rangle\langle 1|, \frac{1}{\sqrt{2}}|+\rangle\langle +|, \frac{1}{\sqrt{2}}|-\rangle\langle -|$$

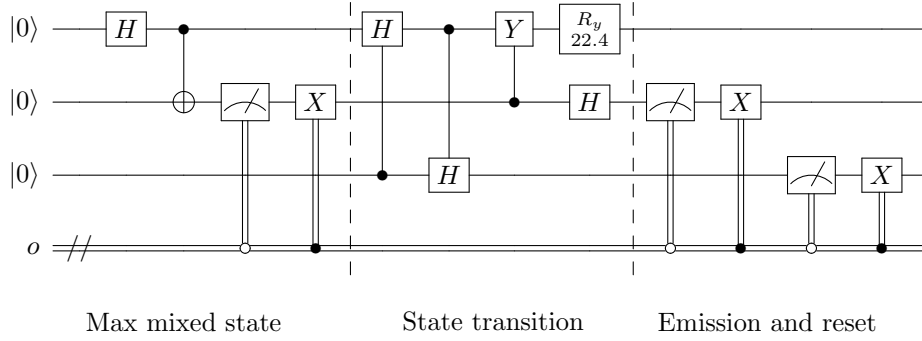


FIG. 20. Gaussian QHMM

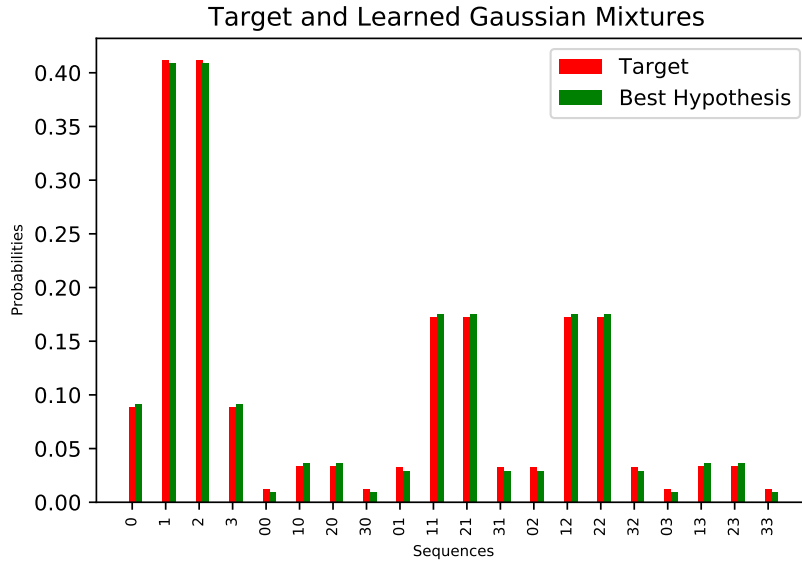


FIG. 21. Learned Gaussian Mixture

or

$$\begin{pmatrix} \frac{1}{\sqrt{2}} & 0 \\ 0 & 0 \end{pmatrix}, \begin{pmatrix} 0 & 0 \\ 0 & \frac{1}{\sqrt{2}} \end{pmatrix}, \frac{1}{2} \begin{pmatrix} \frac{1}{\sqrt{2}} & \frac{1}{\sqrt{2}} \\ \frac{1}{\sqrt{2}} & \frac{1}{\sqrt{2}} \end{pmatrix}, \frac{1}{2} \begin{pmatrix} \frac{1}{\sqrt{2}} & -\frac{1}{\sqrt{2}} \\ -\frac{1}{\sqrt{2}} & \frac{1}{\sqrt{2}} \end{pmatrix}$$

In this case, we will use the maximally mixed state as the start state. Next, we model this sequence using the set of ansatz circuits described in Section III B and compare different entanglement strategies that include full entanglement and linear entanglement. The comparison of the results is presented in Table V.

Clearly, the EfficientSU2 (R_z, R_x) style ansatz performs much better than others. However, there is only marginal difference between full and linear entanglement strategies. Due to the heavy hex lattice

Ansatz	Entanglement	Cost
EfficientSU2 (R_z, R_x)	full	3.90e-5
EfficientSU2 (R_z, R_x)	linear	4.23e-5
RealAmplitudes	full	0.155
RealAmplitudes	linear	0.689
EfficientSU2 (R_y, R_z)	full	0.156
EfficientSU2 (R_y, R_z)	linear	0.155

TABLE V. Optimized cost for different ansatz circuits

used in IBM processors, it is expensive to run the circuit with full entanglement on four qubits. However, we have seen that the use of linear entanglement pro-

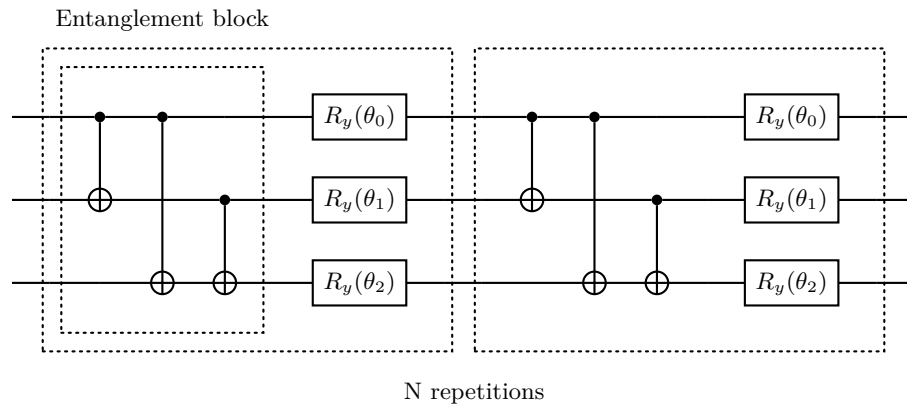
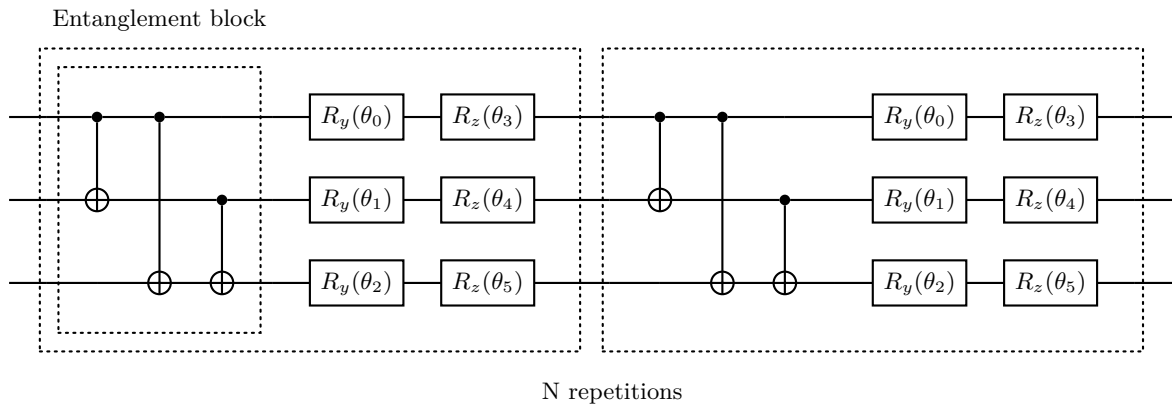
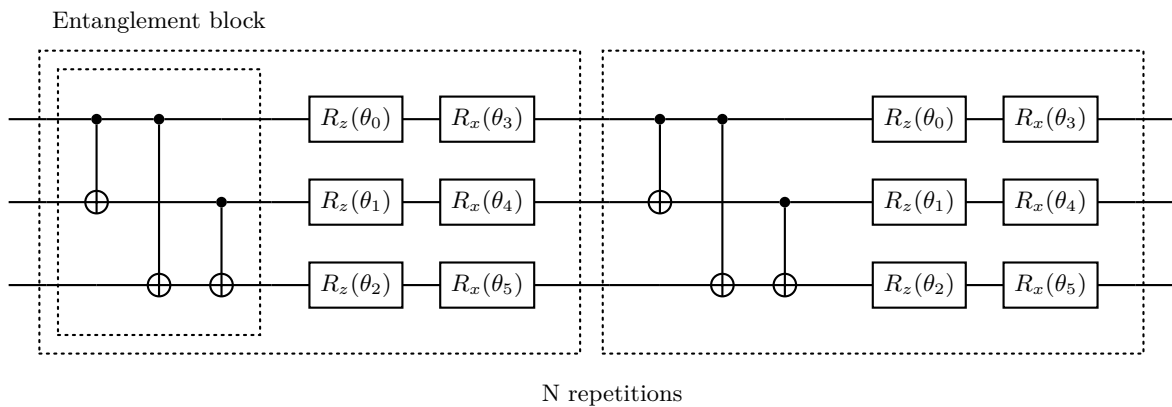


FIG. 22. Real Amplitudes Ansatz Circuit

FIG. 23. EfficientSU2 Ansatz Circuit with R_y and R_z RotationsFIG. 24. EfficientSU2 Ansatz Circuit with R_z and R_x Rotations

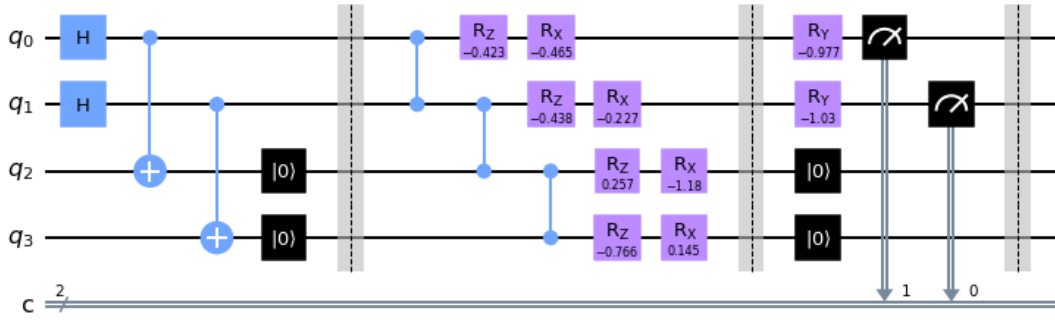


FIG. 25. Circuit for 1 step with optimized parameters

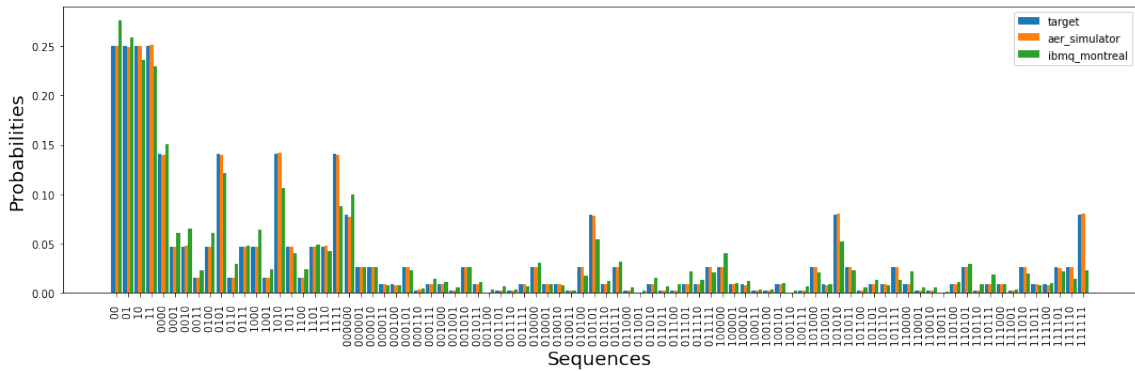


FIG. 26. Predicted and observed probabilities

duces equally good results, so we will proceed with the linear entanglement design FIG 25. The result is presented in FIG 26. Hardware results [75] clearly capture the pattern. However, the current level of hardware noise still seems too high for longer sequences.

The hardware run was executed using *Sampler* primitive on *Qiskit Runtime* with *optimization_level=2* [76, 77].

B. Classic Market Model with Four Hidden States

The process is defined by transition and emission matrices in Table I.

We will simulate this process using 2 qubits: one for the principal system and one for the environment. We will use the maximally mixed state as the initial state. For the main transition unitary, we will use *RealAmplitudes*, *EfficientSU2* (R_y, R_z) and *EfficientSU2* (R_z, R_x) ansatz circuits. Clearly, for the circuit of only 2 qubits linear and full entanglement produce the same result.

Once we train the model following Algorithm 6, we get the following costs associated with the ansatz circuits (Table VI):

TABLE VI. Optimized cost for different ansatz circuits

Ansatz	Cost
<i>EfficientSU2</i> (R_z, R_x)	0.00030
<i>RealAmplitudes</i>	0.00030
<i>EfficientSU2</i> (R_y, R_z)	0.00036

The results are very close, so we can pick the simplest circuit to continue. In this case, we choose *RealAmplitudes* since it has only 2 parameters. The circuit for 1 step with optimized parameters is shown in FIG 27.

Comparison with the hardware run on *ibmq_montreal* using *Qiskit Runtime* and *Sampler* primitive [78] is shown in FIG 28. The hardware run was executed using *Sampler* primitive on *Qiskit Runtime* with *optimization_level = 2* [76, 77].

The training has converged to the final solution very quickly. In fact, it is easy to see that even the *RealAmplitudes* ansatz is too expressive for this

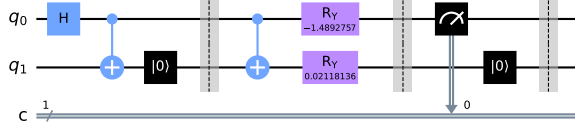


FIG. 27. Circuit for 1 step with optimized parameters

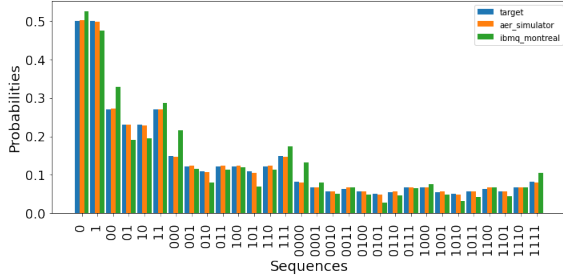


FIG. 28. Predicted and observed probabilities

stochastic process and we can further simplify it by removing R_Y rotation gate on q_1 .

VI. CONCLUSIONS AND OUTLOOK

In this paper, we utilized the theory of open quantum systems to study complexity, unitary implementation, and learning from examples of a class of quantum stochastic generators known as Quantum Hidden Markov Models. We have demonstrated that the integration of unitary dynamics of a principal (or “state”) quantum system, entangled with an emission system (“environment”) where observations are generated through orthogonal measurement, presents a state-efficient model of finite-order stochastic languages. The Markovian behavior of the model’s state evolution is guaranteed by the direction of the information flow from the principal system to the environment. We note that there are other quantum architectures that generate joint evolution of a Markovian state process and a dependent observable process. It is especially important to characterize the processes generated by sequential measurements of cluster state quantum systems [79], [25]. Since these systems have fewer parameters, the general entanglement architecture and the parameters of the measurement basis, we would expect efficient learning algorithms.

Another important research opportunity is to apply the approach developed in the article to devices and processes with non-Markovian behavior. In this case, we need to establish an information flow, or input, from the environment towards the state system [80]. This will allow to model higher-order Hidden Markov Models, finite-state transducers, and generators with attention mechanisms.

We proposed three variational ansatz circuits to be used as a starting point to model classical sequence data and tested on two use cases with 4 hidden states and 2 and 4 observed outcomes.

VII. ACKNOWLEDGEMENTS

We thank Vaibhaw Kumar, Jae-Eun Park, Laura Schleeper, and Rukhsan UI Haq for helpful discussions at the start of this work. We would like to thank John Watrous for his comments regarding quantum channels.

The views expressed in this article are those of the authors and do not represent the views of Wells Fargo. This article is for informational purposes only. Nothing contained in this article should be construed as investment advice. Wells Fargo makes no express or implied warranties and expressly disclaims all legal, tax, and accounting implications related to this article.

-
- [1] S. Karlin and H. Taylor, *A first course in stochastic processes*. Academic press, 2012.
- [2] R. S. Mamon and R. J. Elliott, *Hidden Markov models in finance*, vol. 4. Springer, 2007.
- [3] L. E. Baum and T. Petrie, “Statistical inference for probabilistic functions of finite state Markov chains,” *The annals of mathematical statistics*, vol. 37, no. 6, pp. 1554–1563, 1966.
- [4] L. R. Rabiner, “A tutorial on hidden Markov models and selected applications in speech recognition,” *Proceedings of the IEEE*, vol. 77, no. 2, pp. 257–286, 1989.
- [5] A. Anandika, S. P. Mishra, and M. Das, “Review on usage of hidden Markov model in natural language processing,” in *Intelligent and Cloud Computing: Proceedings of ICICC 2019, Volume 1*, pp. 415–423, Springer, 2021.
- [6] F. Lefèvre, “Non-parametric probability estimation for hmm-based automatic speech recognition,” *Computer Speech & Language*, vol. 17, no. 2-3, pp. 113–136, 2003.
- [7] K. L. Mangi Kang, Jaelim Ahn, “Opinion mining using ensemble text hidden Markov models for text classification,” *Expert Systems with Applications*, vol. 94, pp. 218–227, 2018.
- [8] T. M. Porter and M. Hajibabaei, “Profile hidden Markov model sequence analysis can help remove putative pseudogenes from dna barcoding and metabarcoding datasets,” *BMC bioinformatics*, vol. 22, no. 1, p. 256, 2021.
- [9] C. Yau, O. Papaspiliopoulos, G. Roberts, and C. Holmes, “Nonparametric hidden Markov models with application to the analysis of copy-number-variation in mammalian genomes,” *J R Stat Soc Series B Stat Methodol*, vol. 73, no. 1, pp. 37–57, 2011.
- [10] A. Krogh, M. Brown, I. Mian, K. Sjölander, and D. Haussler, “Hidden Markov models in computational biology. applications to protein modeling,” *J Mol Biol*, vol. 235, no. 5, pp. 1501–1531, 1994.
- [11] J. M. Lee, S.-J. Kim, Y. Hwang, and C.-S. Song, “Diagnosis of mechanical fault signals using continuous hidden Markov model,” *Journal of Sound and Vibration*, vol. 276, no. 3-5, pp. 1065–1080, 2004.
- [12] K. D. Ullah I, Ahmad R, “A prediction mechanism of energy consumption in residential buildings using hidden Markov model,” *Energies*, vol. 11, no. 2, pp. 1–20, 2018.
- [13] Y. Yuan and G. Mitra, “Market regime identification using hidden Markov models,” *SSRN Electronic Journal*, 2019.
- [14] L. E. Baum, T. Petrie, G. Soules, and N. Weiss, “A maximization technique occurring in the statistical analysis of probabilistic functions of Markov chains,” *The annals of mathematical statistics*, vol. 41, no. 1, pp. 164–171, 1970.
- [15] L. E. Baum *et al.*, “An inequality and associated maximization technique in statistical estimation for probabilistic functions of Markov processes,” *Inequalities*, vol. 3, no. 1, pp. 1–8, 1972.
- [16] P. J. Bickel, Y. Ritov, and T. Ryden, “Asymptotic normality of the maximum-likelihood estimator for general hidden Markov models,” *The Annals of Statistics*, vol. 26, no. 4, pp. 1614–1635, 1998.
- [17] L. A. Kontorovich, B. Nadler, and R. Weiss, “On learning parametric-output HMMs,” in *International Conference Machine Learning*, pp. 702–710, 2013.
- [18] S. A. Terwijn, “On the learnability of hidden Markov models,” in *International Colloquium on Grammatical Inference*, pp. 261–268, Springer, 2002.
- [19] B. Ghogh, F. Karray, and M. Crowley, “Hidden Markov model: Tutorial,” 2019.
- [20] B. Anderson, “The realization problem for hidden Markov models,” *Mathematics of Control, Signals and Systems*, vol. 12, no. 1, pp. 80–120, 1999.
- [21] D. Hsu, S. M. Kakade, and T. Zhang, “A spectral algorithm for learning hidden Markov models,” *Journal of Computer and System Sciences*, vol. 78, no. 5, pp. 1460–1480, 2012.
- [22] B. Balle, X. Carreras, F. M. Luque, and A. Quattoni, “Spectral learning of weighted automata,” *Machine learning*, vol. 96, no. 1, pp. 33–63, 2014.
- [23] H. Jaeger, “Observable operator models for discrete stochastic time series,” *Neural computation*, vol. 12, no. 6, pp. 1371–1398, 2000.
- [24] M. A. Nielsen and I. L. Chuang, *Quantum Computation and Quantum Information: 10th Anniversary Edition*. Cambridge University Press, 2010.
- [25] A. Monras, A. Beige, and K. Wiesner, “Hidden quantum Markov models and non-adaptive read-out of many-body states,” *Applied Mathematical and Computational Sciences*, vol. 3, no. 1, pp. 93–122, 2011.
- [26] S. Srinivasan, G. Gordon, and B. Boots, “Learning hidden quantum Markov models,” 2017.
- [27] S. Srinivasan, C. Downey, and B. Boots, “Learning and inference in hilbert space with quantum graphical models,” 2018.
- [28] S. Adhikary, S. Srinivasan, and B. Boots, “Learning quantum graphical models using constrained gradient descent on the stiefel manifold,” 2019.
- [29] S. Adhikary, S. Srinivasan, G. Gordon, and B. Boots, *Expressiveness and Learning of Hidden Quantum Markov Models*, vol. 108 of *Proceedings of Machine Learning Research*, pp. 4151–4161. PMLR, 26–28 Aug 2020.
- [30] S. Srinivasan, S. Adhikary, J. Miller, B. Pokharel, G. Rabusseau, and B. Boots, “Towards a trace-preserving tensor network representation of quantum channels,” *Second Workshop on Quantum Tensor Networks in Machine Learning, 35th Conference on Neural Information Processing Systems (NeurIPS 2021)*, 2021.
- [31] S. Srinivasan, S. Adhikary, J. Miller, G. Rabusseau, and B. Boots, “Quantum tensor networks, stochastic processes, and weighted automata,” 2020.
- [32] S. Srinivasan, *Quantum-inspired Machine Learning*

- with Hidden Quantum Markov Models and Tensor Networks. PhD thesis, 2022.
- [33] B. O’Neill, T. M. Barlow, D. Šafránek, and A. Beige, “Hidden quantum Markov models with one qubit,” *AIP Conference Proceedings*, vol. 1479, no. 1, pp. 667–669, 2012.
- [34] L. A. Clark, W. Huang, T. M. Barlow, and A. Beige, “Hidden quantum Markov models and open quantum systems with instantaneous feedback,” in *ISCS 2014: Interdisciplinary Symposium on Complex Systems*, pp. 143–151, Springer, 2015.
- [35] M. A. Javidian, V. Aggarwal, and Z. Jacob, “Learning circular hidden quantum Markov models: A tensor network approach,” *arXiv preprint arXiv:2111.01536*, 2021.
- [36] M. Cholewa, P. Gawron, P. Głomb, and D. Kurzyk, “Quantum hidden Markov models based on transition operation matrices,” *Quantum Information Processing*, vol. 16, no. 4, pp. 1–19, 2017.
- [37] T. J. Elliott, “Memory compression and thermal efficiency of quantum implementations of nondeterministic hidden Markov models,” *Phys. Rev. A*, vol. 103, p. 052615, May 2021.
- [38] C. Blank, D. K. Park, and F. Petruccione, “Quantum-enhanced analysis of discrete stochastic processes,” *npj Quantum Information*, vol. 7, no. 1, pp. 1–9, 2021.
- [39] W. F. Stinespring, “Positive functions on C*-algebras,” *Proceedings of the American Mathematical Society*, vol. 6, no. 2, p. 211–216, 1955.
- [40] D. Kretschmann, D. Schlingemann, and R. F. Werner, “A continuity theorem for stinespring’s dilation,” *Journal of Functional Analysis*, vol. 255, no. 8, pp. 1889–1904, 2008.
- [41] S. W. Dharmadhikari, “Functions of Finite Markov Chains,” *The Annals of Mathematical Statistics*, vol. 34, no. 3, pp. 1022 – 1032, 1963.
- [42] M. Fox and H. Rubin, “Functions of Processes with Markovian States,” *The Annals of Mathematical Statistics*, vol. 39, no. 3, pp. 938 – 946, 1968.
- [43] H. Jaeger, “Observable operator models for discrete stochastic time series,” *Neural Computation*, vol. 12, no. 6, pp. 1371–1398, 2000.
- [44] J. Carlyle and A. Paz, “Realizations by stochastic finite automata,” *Journal of Computer and System Sciences*, vol. 5, no. 1, pp. 26–40, 1971.
- [45] Q. Huang, R. Ge, S. Kakade, and M. Dahleh, “Minimal realization problem for hidden Markov models,” in *2014 52nd Annual Allerton Conference on Communication, Control, and Computing (Allerton)*, pp. 4–11, 2014.
- [46] M. Vidyasagar, “The realization problem for hidden Markov models: The complete realization problem,” in *Proceedings of the 44th IEEE Conference on Decision and Control*, pp. 6632–6637, 2005.
- [47] E. Sontag, “On some questions of rationality and decidability,” *Journal of Computer and System Sciences*, vol. 11, pp. 375–381, Dec. 1975.
- [48] J.-P. Bouchaud, J. Bonart, J. Donier, and M. Gould, *Trades, Quotes and Prices: Financial Markets Under the Microscope*. Cambridge University Press, 2018.
- [49] I. Bengtsson and K. Życzkowski, *Geometry of Quantum States: An Introduction to Quantum Entanglement*. Cambridge University Press, 2 ed., 2017.
- [50] M.-D. Choi, “Completely positive linear maps on complex matrices,” *Linear Algebra and its Applications*, vol. 10, no. 3, pp. 285–290, 1975.
- [51] M. Vidyasagar, “The complete realization problem for hidden Markov models: a survey and some new results,” *Mathematics of Control, Signals, and Systems*, vol. 23, no. 1, pp. 1–65, 2011.
- [52] H.-P. Breuer and F. Petruccione, *The Theory of Open Quantum Systems*. Oxford University Press, 2007.
- [53] A. Rivas and S. F. Huelga, *Open Quantum Systems*. Springer Berlin, Heidelberg, 2012.
- [54] S. E. Smart, Z. Hu, S. Kais, and D. A. Mazziotti, “Relaxation of stationary states on a quantum computer yields a unique spectroscopic fingerprint of the computer’s noise,” *Communications Physics*, vol. 5, no. 1, p. 28, 2022.
- [55] Á. Rivas, S. F. Huelga, and M. B. Plenio, “Quantum non-Markovianity: characterization, quantification and detection,” *Reports on Progress in Physics*, vol. 77, no. 9, p. 094001, 2014.
- [56] F. A. Pollock, C. Rodríguez-Rosario, T. Frauenheim, M. Paternostro, and K. Modi, “Operational Markov condition for quantum processes,” *Phys. Rev. Lett.*, vol. 120, p. 040405, Jan 2018.
- [57] S. Filippov, G. Semin, and A. Pechen, “Quantum master equations for a system interacting with a quantum gas in the low-density limit and for the semiclassical collision model,” *Physical Review A*, vol. 101, no. 1, p. 012114, 2020.
- [58] J. Morris, F. A. Pollock, and K. Modi, “Non-Markovian memory in ibmqx4,” *arXiv preprint arXiv:1902.07980*, 2019.
- [59] M. M. Wilde, “Preface to the second edition,” in *Quantum Information Theory*, pp. xi–xii, Cambridge University Press, nov 2016.
- [60] “Mid-circuit measurement.” <https://quantum-computing.ibm.com/lab/docs/iql/manage/systems/midcircuit-measurement/>. Accessed: 2022-11-16.
- [61] “Introduction to dynamic circuits.” <https://quantum-computing.ibm.com/admin/docs/admin/manage/systems/dynamic-circuits/Introduction-To-Dynamic-Circuits>. Accessed: 2022-11-16.
- [62] “Qiskit runtime, job cdcu23veprknk3brdl6g.” <https://quantum-computing.ibm.com/runtime/jobs/cdcu23veprknk3brdl6g>. Completed: 2022-10-27.
- [63] “Introducing new qiskit runtime capabilities — and how our clients are integrating them into their use.” <https://research.ibm.com/blog/qiskit-runtime-capabilities-integration>. Accessed: 2022-11-17.
- [64] D. Hsu, S. M. Kakade, and T. Zhang, “A spectral algorithm for learning hidden Markov models,” *Journal of Computer and System Sciences*, vol. 78, no. 5,

- pp. 1460–1480, 2012. JCSS Special Issue: Cloud Computing 2011.
- [65] S. P. Finesso Lorenzo, Grassi Angela, “Approximation of stationary processes by hidden Markov models,” *Mathematics of Control, Signals, and Systems*, vol. 22, pp. 1–22, 2010.
- [66] M. J. Kearns, *The computational complexity of machine learning*. MIT press, 1990.
- [67] D. Aharonov, A. Kitaev, and N. Nisan, “Quantum circuits with mixed states,” in *Proceedings of the thirtieth annual ACM symposium on Theory of computing*, pp. 20–30, 1998.
- [68] A. Holzinger, D. Blanchard, M. Bloice, K. Holzinger, V. Palade, and R. Rabadan, “Darwin, lamarck, or baldwin: Applying evolutionary algorithms to machine learning techniques,” in *2014 IEEE/WIC/ACM International Joint Conferences on Web Intelligence (WI) and Intelligent Agent Technologies (IAT)*, vol. 2, pp. 449–453, 2014.
- [69] S. Sim, P. D. Johnson, and A. Aspuru-Guzik, “Expressibility and entangling capability of parameterized quantum circuits for hybrid quantum-classical algorithms,” *Advanced Quantum Technologies*, vol. 2, no. 12, p. 1900070, 2019.
- [70] M. Aoki, *Notes on Economic Time Series Analysis: System Theoretic Perspectives*. Springer Berlin, Heidelberg, 1983.
- [71] Y. Du, T. Huang, S. You, M.-H. Hsieh, and D. Tao, “Quantum circuit architecture search for variational quantum algorithms,” *npj Quantum Information*, vol. 8, no. 1, pp. 1–8, 2022.
- [72] T. Haug, K. Bharti, and M. Kim, “Capacity and quantum geometry of parametrized quantum circuits,” *PRX Quantum*, vol. 2, no. 4, p. 040309, 2021.
- [73] Z. Holmes, K. Sharma, M. Cerezo, and P. J. Coles, “Connecting ansatz expressibility to gradient magnitudes and barren plateaus,” *PRX Quantum*, vol. 3, no. 1, p. 010313, 2022.
- [74] M. S. A. et al., “Qiskit: An open-source framework for quantum computing,” 2021.
- [75] “Qiskit runtime, job cdrs794godki4idpf4og.” <https://quantum-computing.ibm.com/jobs/cdrs794godki4idpf4og>. Completed: 2022-11-18.
- [76] “Configure error suppression.” https://qiskit.org/documentation/partners/qiskit_ibm_runtime/how_to/error-suppression.html. Accessed: 2022-11-21.
- [77] “Configure error mitigation.” https://qiskit.org/documentation/partners/qiskit_ibm_runtime/how_to/error-mitigation.html. Accessed: 2022-11-21.
- [78] “Qiskit runtime, job cdtbhmge9lpogos7o1vg.” <https://quantum-computing.ibm.com/jobs/cdtbhmge9lpogos7o1vg>. Completed: 2022-11-20.
- [79] H. J. Briegel and R. Raussendorf, “Persistent entanglement in arrays of interacting particles,” *Phys. Rev. Lett.*, vol. 86, pp. 910–913, Jan 2001.
- [80] H.-P. Breuer, E.-M. Laine, and J. Piilo, “Measure for the degree of non-Markovian behavior of quantum processes in open systems,” *Phys. Rev. Lett.*, vol. 103, p. 210401, Nov 2009.